The influence of host immunity on outcomes following hormone therapy for cancer

by

Sara Hahn
BSc., University of Guelph, 2005

A Thesis Submitted in Partial Fulfillment
of the Requirements for the Degree of

MASTER OF SCIENCE

in the Department of Biochemistry and Microbiology

Supervisory Committee

The influence of host immunity on outcomes following hormone therapy for cancer

by

Sara Hahn
BSc., University of Guelph, 2005

Supervisory Committee

Dr. Brad H. Nelson, (Department of Biology)
Supervisor

Dr. Terry Pearson, (Department of Biochemistry and Microbiology)
Co-Supervisor or Departmental Member

Dr. Perry Howard, (Department of Biochemistry and Microbiology)
Departmental Member

Dr. Rob Ingham, (Department of Biology)
Outside Member

Abstract

Supervisory Committee
Dr. Brad H. Nelson, (Department of Biology)
Supervisor
Dr. Terry Pearson, (Department of Biochemistry and Microbiology)
Co-Supervisor or Departmental Member
Dr. Perry Howard, (Department of Biochemistry and Microbiology)
Departmental Member
Dr. Rob Ingham, (Department of Biology)
Outside Member

BACKGROUND: We have recently shown that standard treatments for prostate cancer, specifically hormone therapy (HT) and radiation therapy, induce antigen-specific immune responses in human patients. However, the contribution of these antigen-specific immune responses to clinical outcomes is not known.

HYPOTHESIS: HT induces tumour-specific antibody and T cell responses that delay or prevent tumour recurrence.

METHODS: We utilized the androgen-dependent Shionogi tumour cell line. Male DD/S mice bearing established Shionogi tumours (~64 mm^2) were castrated to induce tumour regression, similar to HT in human prostate cancer patients. Control mice were not castrated. Mice were monitored for tumour recurrence. Tumour-specific antibody responses were measured by immunoblot, and T cell responses by ELISPOT and immunohistochemistry. Tumour-specific antigens were identified by serological screening of a cDNA expression library (SEREX).

RESULTS: Following castration, 32/33 mice experienced complete tumour regression, while the remaining mouse experienced partial tumour regression. Of the 32 mice that underwent complete regression, 72% (23/32) experienced tumour recurrence 3-70 days post-castration, while the remaining 28% (9/32) remained tumour-free for the duration of the experiment until they were sacrificed for analysis (64-86 days post-castration). Shionogi tumours became heavily infiltrated by CD3+ T cells between 7-14 days post-castration, after which T cell infiltrates became progressively more sparse. Castration induced antibody responses to one or more tumour proteins in approximately one third of mice with an average latency of 21 days. The most common antibody response was

against poly(A) binding protein, nuclear 1 (PABPN1). Interestingly, 71% (17/24) of mice with recurrent tumours had an antibody response against PABPN1, whereas only 11% (1/9) of mice that remained tumour-free had a PABPN1-specific antibody response. Put another way, the mean tumour-free interval for those mice that had a PABPN1 antibody response was approximately 25 days compared to approximately 63 days for those mice that did not have a PABPN1 antibody response. However, we found a moderate correlation between the timing of the PABPN1-specific antibody response and growth rate of the recurrent tumour, such that if a mouse had a PABPN1-specific antibody response that occurred shortly after castration, it was more likely to have a slower growing recurrent tumour. IFN-γ ELISPOT assays revealed that castration also induced a PABPN1-specific T cell response that persisted for the duration of the experiment (up to 92 days post-castration). Unexpectedly, this T cell response was exceedingly stronger in recurrent mice versus non-recurrent mice and was accompanied by splenomegaly in recurrent mice. Anti-CD3 staining of the recurrent tumours showed that the CD3+ T cells were confined to the periphery and stroma of the tumours.

CONCLUSIONS: In the androgen-dependent murine Shionogi carcinoma model, HT induces robust antibody and T cell responses to PABPN1 that are associated with unfavourable outcomes. To determine why those mice that do not have PABPN1-specific antibody and T cell responses have better outcomes, we will further delineate the T cell response with respect to CD4+ versus CD8+ subpopulations. Additionally, we will investigate the use of immunomodulatory agents to amplify host CD8+ T cell responses and thereby improve the therapeutic effects of HT.

Table of Contents

List of Figures

Abbreviations

AP	alkaline phosphatase
APC	antigen presenting cell
BCA	bicinchoninic acid
BCIP	5-bromo-4-chloro-3-indolyl phosphate
BSA	bovine serum albumin
cDNA	complementary deoxyribonucleic acid
CEP78	centrosomal protein 78kDa
CNBr	cyanogen bromide
conA	concanavalin A
CRNKL1	crooked neck-like 1
DMSO	dimethyl sulfoxide
DNA	deoxyribonucleic acid
DTT	dithiothreitol
EBRT	external beam radiation therapy
ECL	enhanced chemiluminescence
FACS	fluorescence-activated cell sorting
FBS	fetal bovine serum
FITC	fluorescein isothiocyanate
FOXP3	forkhead box P3
GAPDH	glyceraldehyde 3-phosphate dehydrogenase
GM-CSF	granulocyte macrophage colony-stimulating factor

H&E	hematoxylin and eosin
HRP	horseradish peroxidase
HRPC	hormone refractory prostate cancer
HT	hormone therapy
IFA	incomplete Freund's adjuvant
IFN-γ	gamma interferon
IgG	immunoglobulin G
IHC	immunohistochemistry
IMAC	immobilized metal ion adsorption chromatography
IPTG	isopropyl β-D-1-thiogalactopyranoside
kDa	kilodaltons
LB	luria broth
MDH	malate dehydrogenase
MHC	major histocompatability complex
mRNA	messenger ribonucleic acid
NBT	nitroblue tetrazolium
NCBI	National Center for Biotechnology Information
OD	optical density
ODF2	outer dense fiber of sperm tails 2
PABPN1	poly(A) binding protein, nuclear 1
PAP	prostatic acid phosphatase
PARP1	poly (ADP-ribose) polymerase family, member 1
PBS	phosphate buffered saline

PCR	polymerase chain reaction
PE	phycoerythrin
PerCP	peridinin chlorophyll protein
polyI:C	polyinosinic:polycytidylic acid
PSA	prostate-specific antigen
PSMA	prostate-specific membrane antigen
RNA	ribonucleic acid
SDCCAG1	serologically defined colon cancer antigen 1
SDS-PAGE	sodium dodecyl sulfate polyacrylamide gel electrophoresis
SEREX	serological identification of antigens by recombinant cDNA expression cloning
SH3GLB1	SH3-domain GRB2-like endophilin B1
TAA	tumour-associated antigen
TBS	Tris-buffered saline
TBST	Tris-buffered saline-tween-20
T_{H1}	T helper1
T_{H2}	T helper2
ZNF707 + PTMA	zinc finger protein 707 + prothymosin, alpha

Acknowledgments

I would like to express my gratitude to my supervisor, Dr. Brad Nelson, whose expertise, patience, and encouragement motivated me throughout my graduate studies. His exceptional leadership and direction kept me focused and he continually challenged me to think for myself, which allowed me to mature as a young scientist. I greatly appreciate his assistance in writing this thesis. I would like to thank the other members of my committee, Dr. Terry Pearson, Dr. Perry Howard, and Dr. Rob Ingham for their assistance and valuable suggestions they provided me throughout my graduate studies. Finally, I would like to thank Dr. Brian Christie for taking time out from his busy schedule to serve as my external examiner.

I would also like to acknowledge Mary Bowden and Rob Drapala from the Jack Bell Research Centre in Vancouver, BC for their tremendous technical assistance.

A very special thanks to my fellow graduate students and co-workers, especially Nancy Nesslinger, at the Deeley Research Centre, who are truly the friendliest and most generous people I have ever worked with. My graduate experience would not have been as enjoyable and memorable without them. I would also like to acknowledge Katy Milne for preparing and staining the Shionogi tumours for histological analysis.

In conclusion, I recognize that this research would not have been possible without the financial assistance of NSERC (CGS M), the University of Victoria Faculty of Graduate Studies (President's Research Scholarship, Edythe Hembroff-Schleicher Scholarship), and the Department of Biochemistry & Microbiology at the University of Victoria (Teaching Assistantships).

Introduction

Prostate cancer is the most frequently diagnosed cancer in North American men and despite improvements in early detection due to prostate-specific antigen (PSA) screening, it remains the second leading cause of cancer-related death among men (1, 2). The current standard treatments for high-risk localized prostate cancer include neoadjuvant hormone therapy (HT) combined with external beam radiation therapy (EBRT) or brachytherapy (3). While these treatments are highly effective for localized disease, the mainstay of treatment for metastatic prostate cancer is HT. Hormone therapy involves the administration of drugs that reduce circulating levels of androgens or that competitively inhibit the action of androgen at the androgen receptor (4). Unfortunately, the majority of patients eventually become resistant to HT, developing hormone-refractory prostate cancer (HRPC). The standard of care for HRPC is docetaxel chemotherapy, which has limited survival benefits and considerable toxicities (4-6). Recent advances in the understanding of cancer immunology have stimulated considerable interest in utilizing cancer immunotherapy to further improve clinical outcomes, especially for those patients with metastatic HRPC (7). The importance of the immune system for recognizing and destroying cancer cells, a process known as cancer immunosurveillance, is well established in mice, as several published studies have shown that mice that lack essential components of the innate and/or adaptive immune system are more susceptible to the development of spontaneous or chemically induced tumours (8). Essentially, immunotherapeutic strategies involve stimulating components of the patient's innate and/or adaptive immune system to recognize tumour-specific antigens,

ultimately resulting in the eradication of the tumour cells expressing these antigens. One major advantage of immunotherapy is that it targets tumour-associated antigens (TAAs), thus for the most part, normal cells are left unharmed, resulting in minimal treatment-related toxicities. Unfortunately, a drawback and limiting factor in the development of immunotherapeutics is that TAAs are usually not cancer-specific, but rather self-antigens that are over-expressed. Since the immune system has already been exposed to these self-antigens, they are not readily recognized as foreign and thus are often only weakly immunogenic (6, 9). However, prostate cancer is one of a few types of cancer where a number of highly tissue-specific antigens have been identified. The three main antigens that have been exploited for prostate cancer immunotherapy are PSA, which is also used as a marker for disease burden, prostate-specific membrane antigen (PSMA), and prostatic acid phosphatase (PAP). In addition to their tissue-specificity, these prostate cancer-associated self-antigens are typically over-expressed in malignant disease, which helps overcome the issue of immune tolerance (2, 6). Prostate cancer is also a good target for immunotherapy due to the slow rate at which prostate tumour cells typically grow. This allows time for the stimulated immune system to mount anti-tumour responses (7). One immunotherapeutic approach that is currently being tested in late stages of clinical trials on prostate cancer patients is GVAX®, which consists of two inactivated allogeneic prostate cancer cell lines (PC-3 and LNCaP) that have been genetically modified to secrete granulocyte macrophage colony-stimulating factor (GM-CSF). GM-CSF is a cytokine that strongly promotes dendritic cell activation and migration and it also participates in the initiation of danger signals needed to activate the immune system (10). Thus far, phase II clinical trials in patients with metastatic HRPC

have shown that treatment with GVAX® lowered serum PSA transiently, as well as extended the time to clinical progression (5). Another novel immunotherapeutic agent currently being evaluated in phase III clinical trials is Provenge®. This vaccine is derived from autologous dendritic cells pulsed *ex vivo* with a recombinant fusion protein consisting of GM-CSF and PAP. Provenge® has shown significant activity in two phase II clinical trials in men with androgen-dependent biochemically relapsed prostate cancer, where it has been shown to cause a decrease in PSA and prolongation of PSA doubling time (5, 6, 11). Furthermore, in a phase III clinical trial, Provenge® induced PAP-specific T cell responses and significantly increased 3-year overall survival in patients randomized to Provenge® compared to placebo (25.9 versus 21.4 months, p=0.01), representing the first survival advantage attributable to an immunotherapy product in prostate cancer (6, 12). Overall, the encouraging results from late-phase clinical testing with these immunotherapeutic approaches have generated tremendous excitement and hope with respect to improving clinical outcomes for patients with metastatic HRPC (2, 5).

While the next frontier of cancer therapy has largely focused on immunotherapeutic strategies, there is little information available on whether standard treatments might also induce tumour-specific immune responses. For instance, HT induces apoptosis of hormone-dependent prostate tumour and epithelial cells, and in turn, the apoptotic bodies can potentially serve as an efficient source of antigen to prime antigen presenting cells (APCs) (13). Similarly, EBRT has been shown to up-regulate a number of immunoregulatory molecules, including chemokines; inflammatory cytokines involved in cell-mediated immunity (14); Fas/CD95 and other death receptors; major

histocompatability complex (MHC) molecules; B7 and other co-stimulatory molecules; adhesion molecules; heat shock proteins; and TAAs (15-18). Therefore, one can imagine that HT and EBRT, by causing tumour cell death in an inflammatory context, may have an impact on the host immune response. A number of studies have provided evidence that the immune system is capable of recognizing tumour antigens. For example, McNeel *et al.* (19) found that antibody responses to PSA and HER-2/neu were significantly higher in prostate cancer patients compared to male controls. Additionally, a study by Wang *et al.* (20) found that patients with prostate cancer, who had received no previous prostate cancer therapy, produced antibodies against a variety of antigens derived from prostate cancer tissue. Likewise, Hoeppner *et al.* (1) found that sera from prostate cancer patients recognized several antigens with a predominantly testis-specific expression in normal tissues. While these studies provided evidence that prostate tumours are recognized by the immune system in a significant proportion of patients, only a couple of studies have shown that standard treatments lead to the induction of tumour-specific immune responses. Mercader *et al.* (13) demonstrated that androgen withdrawal induced profuse T cell infiltration of benign prostate glands and tumours. Following HT, this study also demonstrated increasing levels of APCs, along with a rise in the T cell co-stimulatory molecules B7.1 and B7.2, which combined with increasing sources of antigen, likely led to the T cell infiltration of the prostate that was observed (13). The mechanism by which T cells traffic to and persist in the prostate is unclear, although one possibility could be the expression of chemoattractant molecules in the tumour microenvironment (21). Regardless of the exact mechanism, tumours of various origin, including prostate, that are densely infiltrated by T cells have been shown to be

associated with favourable outcomes relative to those tumours with absent or decreased T cell infiltrates (22-25). Recently, Nesslinger *et al.* (26) were the first to show that standard treatments induce antigen-specific immune responses in prostate cancer patients. In this study, immunoblotting revealed the development of treatment-associated antibody responses in patients undergoing neoadjuvant HT (7 of 24, 29.2%), EBRT (4 of 29, 13.8%), and brachytherapy (5 of 20, 25%), compared with 0 of 14 patients undergoing radical prostatectomy and 2 of 36 (5.6%) controls. Furthermore, Nesslinger *et al.* (26) utilized serological identification of antigens by recombinant cDNA expression cloning (SEREX) immunoscreening of a prostate cancer cDNA expression library and identified several antigens, including poly (ADP-ribose) polymerase family, member 1 (PARP1), zinc finger protein 707 + prothymosin, alpha (ZNF707 + PTMA), centrosomal protein 78kDa (CEP78), serologically defined colon cancer antigen 1 (SDCCAG1), and outer dense fiber of sperm tails 2 (ODF2), that were recognized by treatment-associated antibodies in four patients. Despite the reports by Mercader *et al.* (13) and Nesslinger *et al.* (26) showing that standard treatments induce immune responses in prostate cancer patients, it is not yet known how these immune responses influence outcomes.

SEREX

The advent of SEREX methodology in 1995 by Sahin *et al.* (27) represented a major advancement in immunoscreening because it allowed the identification of biomarkers and tumour antigens of clinical significance for cancer diagnosis, prognosis, and therapy (28-30). This methodology involves using sera from cancer patients to screen cDNA expression libraries derived from human tumours or cancer cell lines, thus resulting in the identification of recombinant tumour antigens by immunoglobulin G

(IgG) antibodies present in the patient's serum (9). Since antibodies are stable and abundant, even at low tumour burden in the early stages of disease, detection of serum antibody responses to tumour antigens is considered to be a reliable tool (30). To date, over 2,500 tumour antigens have been identified using SEREX, one-third of which are novel, from a variety of malignancies. These antigens can be classified into several categories, including TAAs, differentiation antigens, mutated antigens, cancer-related autoantigens, splice variant antigens, and cancer-testis antigens (29). Overall, SEREX has been extensively used within the last decade to identify a number of proteins related to tumourigenesis. Several modifications to the original SEREX methodology have been introduced to further improve the high-throughput efficiency of the technique and its potential for identifying relevant tumour antigens (28, 30).

Murine Shionogi carcinoma model

The androgen-dependent murine Shionogi carcinoma model (SC-115) was first described in 1965 by Minesita and Yamaguchi. The transplantable androgen-dependent mammary tumour was originally derived from a spontaneous hormone-independent mammary tumour found in a breeder mouse of the DD/Sio strain. Transplantation tests showed that the original tumour grew well in both sexes and as the tumour was serially transplanted through only male mice, the growth rate of the tumour increased and the survival time of the host shortened. At the 19th passage generation, the authors found that the tumour no longer took in female mice nor castrated males, thus indicating that the tumour cells were entirely androgen-dependent (31). Despite the fact that this model is a mouse mammary carcinoma, it is well-characterized and has been used extensively to study the conversion from androgen-dependent to androgen-independent neoplasia.

Initially, Shionogi tumours are androgen-dependent and hence are grown in male mice. Castration, which mimics HT, precipitates apoptosis and tumour regression in a highly reproducible manner, similar to that seen after androgen withdrawal in human prostate cancer patients. However, the androgen-depleted environment invariably gives rise to recurrent tumours with an androgen-independent phenotype, thus mimicking the pattern commonly seen in human prostate cancer (31-33). Furthermore, in an androgen-depleted environment, Shionogi tumour cells that survive hormone withdrawal, like human prostate tumour cells, up-regulate proteins implicated in cell survival and acceleration of tumour progression to androgen independence (32). Bruchovsky *et al.* (34) proposed that the androgen-independent phenotype of recurrent Shionogi tumours may result from the ability of a small number of initially androgen-dependent stem cells to adapt to an altered hormone environment. The androgen-independent recurrent Shionogi tumour arises in the same region where the primary tumour was implanted. Although metastatic lung lesions have been observed in non-castrated male DD/S mice 30 to 40 days post-tumour implantation, no studies have reported the presence of metastatic lesions in castrated male DD/S mice with androgen-independent recurrent tumours (35). Presumably, if castrated male DD/S mice were kept alive for an extended period following the outgrowth of the androgen-independent recurrent Shionogi tumour, metastatic lung lesions might also be found. Finally, Nesslinger *et al.* (26) showed that castration induces an antibody response to a ~40 kDa antigen in approximately 50% of tumour-bearing mice. Thus, the murine Shionogi carcinoma model provides an experimental system for studying the relationship between treatment-induced immune responses and tumour recurrence.

Purpose and hypothesis

We recently showed that standard treatments for prostate cancer induce tumour-specific antibody responses in a significant proportion of human patients (26). However, it is not yet known whether these treatment-induced antibody responses influence clinical outcomes since the majority of human prostate cancer patients remain tumour-free for many years following an initial course of therapy. Therefore, we set out to answer this question using a mouse model because we could determine outcomes within a much shorter time frame. Furthermore, using a mouse model allowed us to establish the time course of the immune response following treatment, as well as determine the subsets of lymphocytes that are involved in these tumour-specific immune responses. We utilized the murine Shionogi carcinoma model because we observed in our preliminary experiment that like human prostate cancer patients, treatment, in the form of castration, induced antibody responses in male mice bearing Shionogi tumours. We hypothesized that in the murine Shionogi carcinoma model, castrated DD/S mice that mount treatment-induced tumour-specific immune responses will have delayed tumour recurrence and prolonged survival relative to those mice that do not mount treatment-induced tumour-specific immune responses.

Materials and Methods

SEREX screening of a human prostate cancer phage cDNA expression library

In 2004, a human prostate cancer phage cDNA expression library was constructed at the Deeley Research Centre by Nancy Nesslinger with a total of 5.0 µg mRNA from three human prostate cancer cell lines (LNCaP, PC3, and DU-145) using the ZAP cDNA library construction kit (Stratagene, La Jolla, CA). The LNCaP and PC3 cell lines were purchased from the American Type Culture Collection (Manassas, VA), and the DU-145 cell line was a kind gift from Dr. Ralph deVere White (University of California, Davis Medical Centre, Davis, CA). The library contained 6.8×10^5 clones with a 98.6% recombination frequency (26).

To reduce background during SEREX screening, serum samples were pre-cleared of proteins that might have cross-reacted with *Escherichia coli* XL1-Blue MRF' bacterial proteins. XL1-Blue MRF' protein lysate was prepared by growing a 200 ml culture to OD_{600}=0.5, sonicating the bacteria, and quantifying the XL1-Blue MRF' protein using the Bicinchoninic Acid (BCA) protein assay (Sigma-Aldrich, Oakville, ON). The XL1-Blue MRF' protein lysate was then cross-linked to CNBr-activated resin (Pfizer, Kirkland, QC). To pre-clear the mouse serum, an equal volume of XL1-Blue cross-linked resin and mouse serum were mixed and incubated overnight. The next day the pre-cleared serum was recovered using a Micro Bio-Spin Chromatography column (BioRad, Mississauga, ON) and stored at a 1/20 dilution in 1x Tris-buffered saline (TBS) + 0.05% thimerasol for future use.

To screen the prostate cancer phage cDNA expression library, an overnight culture of XL1-Blue MRF' was grown in 50 ml LB + supplements (10 mM $MgSO_4$, 0.2% maltose) + 15 µg/ml tetracycline. The bacteria were prepared by centrifugation at 1000x g for 10 minutes, re-suspended in 10 mM $MgSO_4$ to obtain OD_{600}=0.5, and then 200 µl were combined with a 2 µl aliquot of the prostate cancer phage cDNA expression library at a 10^{-4} dilution. Following a 15 minute incubation at 37ºC, 3 ml of top agar was added to the bacterial/phage library mixture and poured over a pre-warmed NZYCM plate. After the plates incubated for 3-4 hours at 37 ºC, an isopropyl β-D-1-thiogalactopyranoside (IPTG)-soaked nitrocellulose membrane was placed on top of the agar and the plates were incubated at 37 ºC overnight. The next day, the membranes were carefully peeled off the plates, washed twice in 1x TBS-Tween-20 (TBST) and once in 1x TBS for 5 minutes each, and then blocked with 1x TBS + 1% bovine serum albumin (BSA) for 1 hour. The pre-cleared serum was diluted to 1/400 in 1x TBS + 1% BSA and then pseudo-lifted twice (1 hour per pseudo-lift) against membranes containing non-recombinant phage plaques to help further reduce the background. Once the pre-cleared serum was pseudo-lifted, it was poured over the membranes containing the prostate cancer phage plaques and rocked overnight at room temperature. SEREX screening of the prostate cancer library was performed using serum from a total of 4 mice. Initially, 70 membranes were screened with serum from a single mouse, and then 10 membranes were screened with sera from 3 mice, each represented at a 1/400 dilution. Following the overnight incubation of the membranes with the serum, the membranes were washed twice with 1x TBST and once with 1x TBS for 5 minutes each, and then blocked with 1x TBS + 1% BSA for 1 hour. The secondary antibody, donkey anti-mouse

IgG alkaline phosphatase-conjugated (Jackson ImmunoResearch Laboratories, West Grove, PA), was diluted 1/5,000 in 1x TBS + 1% BSA and added to the membranes. One hour later, the membranes were again washed twice in 1x TBST and once in 1x TBS for 5 minutes each and then developed in nitroblue tetrazolium (NBT)/5-bromo-4-chloro-3-indolyl phosphate (BCIP). After washing the developed membranes in dH_2O for 15 minutes, the membranes were dried and positive clones identified as dark purple spots. The membranes were superimposed on the original plates to identify and core the positive plaques, which were stored in 500 µl SM buffer + 20 µl chloroform. Secondary screens of the positive plaques were performed to ensure the clone was indeed positive and so that a well-isolated core could be chosen. Once the secondary screen confirmed which cored plaques were positive, the phage clones were converted to a plasmid by combining 200 µl XL1-Blue MRF' cells (OD_{600}=1.0) with 250 µl phage stock (from the cored positive clone) and 1 µl ExAssist helper phage. The mixture was incubated for 15 minutes at 37 ºC and then 3 ml LB + supplements was added and incubated for 2.5-3 hours at 37 ºC. Heating the mixture at 70 ºC for 20 minutes lysed the phage particles and cells, which was then centrifuged and the phage supernatant poured into a fresh tube. The phage supernatant (0.1 µl) was mixed with 200 µl *E. coli* SOLR cells (OD_{600}=1.0), incubated for 15 minutes at 37 ºC, and then plated onto LB + ampicillin plates, which were incubated overnight at 37 ºC. Two isolated colonies from each transformation plate were picked and used to inoculate 5 ml LB + 0.1 mg/ml ampicillin, which was grown overnight at 37 ºC, 250 rpm. The next day, plasmids from the overnight cultures were isolated using the QIAprep Spin Miniprep kit (Qiagen, Mississauga, ON) following the manufacturer's directions. Purified plasmid DNA was then digested with KpnI and SacI

to check the insert size (inserts are cloned in pBluescript, which is 3.0 kb). Plasmids containing cloned antigens were sent to the DNA sequencing facility at the University of Victoria. To reveal the identity of the antigen, the DNA sequences were analyzed using NCBI Blast.

Cloning and purification of SEREX-identified antigens

For each of the antigens identified by SEREX screening, forward and reverse primers (obtained from Integrated DNA Technologies, San Diego, CA) were designed such that the entire DNA coding sequence would be amplified by polymerase chain reaction (PCR). Total RNA was extracted from 10 x 10^6 Shionogi tumour cells using the RNeasy Mini kit (Qiagen) and then 0.08 µg total RNA was synthesized into cDNA using SuperScript™ II Reverse Transcriptase (Invitrogen, Burlington, ON). The cDNA was used as a template to amplify each of the SEREX-identified antigens by PCR. The PCR product was run on a 1% agarose gel at 100 V for 45 minutes and then visualized under ultraviolet light to identify the band of interest, which was subsequently cut out of the gel and purified using the QIAquick Gel Extraction kit (Qiagen). The gel-extracted PCR product was then cloned into pENTR™/D-TOPO® (Invitrogen) and transformed into One Shot® TOP10 chemically competent *E. coli* (Invitrogen). Multiple clones from the transformation plate were picked and grown in 5 ml LB + 50 µg/ml kanamycin overnight at 37 ºC, 250 rpm. Plasmid DNA from each clone was extracted using the QIAprep Spin Miniprep kit (Qiagen) and then a 5 µl aliquot was used in a restriction digest to identify clones of interest, which were sent to the DNA sequencing facility at the University of Victoria. Once the DNA sequences were analyzed and it was verified that the antigen of interest was properly cloned into the pENTR™/D-TOPO® vector, it was sub-cloned into

pDEST™ 17 (Invitrogen), an *E. coli* expression vector containing a histidine tag. To verify that the cloning reaction was successful, multiple pDEST™ 17 clones were picked from the transformation plate, grown overnight in 5 ml LB + 0.1 mg/ml ampicillin, and the plasmid DNA was purified and restriction digested. Clones of interest, which were identified by visualizing the expected product sizes from the restriction digest on a 1% agarose gel, were then transformed into BL21-AI™ chemically competent cells (Invitrogen), an *E. coli* strain ideal for expression. For optimal protein production, transformed BL21-AI™ were grown to OD_{600}=0.5 in 400 ml LB + 1 μg/ml ampicillin and then 4 ml of 20% arabinose were added to induce protein production. Two hours later, the bacteria were harvested, centrifuged, and the pellet re-suspended in 5 ml of 30 mM Tris-HCl, pH 7.5, 500 mM NaCl, 20 mM imidazole, and 1 mM dithiothreitol (DTT). After one freeze-thaw cycle at -80 ºC, the re-suspended bacteria were sonicated and then centrifuged. The supernatant, containing soluble protein of interest, was transferred to a new Falcon tube. The pelleted bacterial lysate was re-suspended in 5 ml of 6 M Urea, 30 mM Tris-HCl, pH 7.5, 500 mM NaCl, and 20 mM imidazole and vigorously vortexed every 5 minutes for a 20-minute period. After centrifugation, the supernatant containing insoluble protein of interest was transferred to a new Falcon tube. To determine which fraction contained the largest quantity of protein, a small aliquot of the soluble and insoluble protein fractions were run on a NuPAGE® Novex 4-12% 17-well Bis-Tris gel (Invitrogen) and visualized with Coomassie brilliant blue dye. The fraction containing the largest quantity of protein was subsequently loaded onto a HiTrap IMAC FF nickel column (GE Healthcare, Piscataway, NJ) and purified by immobilized metal ion adsorption chromatography (IMAC) using the ÄKTAprime™ plus (GE Healthcare). The

protein was eluted from the nickel column by using an imidazole gradient. The fractions containing protein, as determined by running eluates on a SDS-PAGE gel, were pooled and dialyzed against 2 L of phosphate buffered saline (PBS) overnight at 4ºC.

Establishing the time course of the immune response in the murine Shionogi carcinoma model

Sixty adult male DD/S mice (bred within the facilities at the Jack Bell Research Centre, Vancouver, BC) were injected subcutaneously with approximately 5 x 10^6 Shionogi carcinoma cells into the neck region. Eleven days later, 50 tumour-bearing mice were castrated to simulate androgen deprivation-type hormone therapy, causing the tumours to regress. The remaining 10 tumour-bearing mice were not castrated and served as the "no treatment" control group. These mice were sacrificed when the primary tumour reached a size approximately equal to 10% of the animal's total body weight. Blood samples were collected from the tail vein of each mouse before tumour inoculation and castration, and then twice weekly following castration. The blood samples were centrifuged and the serum was stored at -80 ºC for future use in immunoblotting assays to determine the proportion of mice with antibody responses. Tumour size (length x width) was measured using microcalipers before castration, and then once per week thereafter. Following castration, 10 mice were sacrificed on days 7, 14, 28, and 35, while the remaining 10 mice were sacrificed when the recurrent tumour reached a size approximately equal to 10% of the animal's total body weight. These time points for sacrifice were chosen based on well-established characteristics of the murine Shionogi carcinoma model, in that by day 14 post-castration the tumour has fully regressed, following which the androgen-independent tumour recurs around day 21-28 post-

castration (32, 33). At the time of sacrifice, a cardiac puncture was performed and the tumour removed, half of which was flash frozen in liquid nitrogen and the other half submerged in 10% formalin. Certain lymph nodes (axillary, inguinal, brachial, mediastenial, and mesenteric) and the spleen were removed from the mouse and pulverized into a single cell suspension using the blunt end of a 5 mm syringe and a 40-μm cell strainer. The splenocytes were re-suspended in ACK lysis buffer (0.15 M NH_4Cl, 1 mM $KHCO_3$, 0.1 mM EDTA, pH 7.3) to lyse the red blood cells. The lymphocytes and splenocytes were then combined, counted using trypan blue and a hemocytometer, and then re-suspended in freezing media (10% dimethyl sulfoxide (DMSO)/90% fetal bovine serum (FBS)). The entire cell suspension was aliquoted into 2 ml cryovials, which were then placed into a Mr. Frosty (VWR International, Mississauga, ON) and frozen at -80 ºC. The next day, the tubes were transferred into a -190 ºC vapour nitrogen freezer for long-term storage.

Histological and immunohistochemical analyses of Shionogi tumours

Formalin-fixed Shionogi tumours were processed following standard methods and stained with hematoxylin and eosin (H&E). A tissue microarray of all the tumours was constructed in duplicate using a 1 mm punch and stained with mouse monoclonal antibodies against CD3 (Lab Vision, RM9107), forkhead box P3 (FoxP3) (eBioscience, 14-5773), Pax-5 (Lab Vision, Rb9406), and granzyme B (Abcam, ab4059).

Criteria for scoring the density of CD3+ T cells within Shionogi tumours

Anti-CD3 stained Shionogi tumours were scored by two individuals who were blinded to the experimental groups. The tumours were examined under a light

microscopy magnification of 200x. A score of "0" was assigned to a tumour that did not contain any CD3+ T cells. A score of "1" was assigned to a tumour that contained a low number of infiltrating CD3+ T cells, while scores of "2" and "3" were assigned to tumours that were moderate to densely infiltrated, respectively. The scores assigned by the two individuals were averaged, unless the difference between the scores was >1, in which case they were discarded for that tumour.

Preparation of tumour lysates for immunoblotting

Cytoplasmic protein lysate was made from intact Shionogi tumours obtained from 5 non-castrated control mice. Using a mortar and pestle, the frozen tumours were pulverized into a fine powder in liquid nitrogen. The powder was re-suspended in 1.5 ml of lysis buffer (1x Dulbecco's PBS, 0.01% Triton, protease inhibitor cocktail) and homogenized using a syringe and 18G and 21G needles. After sonication and centrifugation, the concentration of the protein lysate was determined using the BCA protein assay. Aliquots containing 400 µg of protein lysate were then stored at -80 ºC for future use.

To prepare an aliquot of protein lysate for a SDS-PAGE gel, 75 µl of NuPAGE® LDS Sample Buffer (4x) (Invitrogen) and 30 µl NuPAGE® Sample Reducing Agent (10x) (Invitrogen) were added and then dH_2O was used to bring the total volume to 300 µl. After the sample was incubated at 95 ºC in a heat block for 5 minutes, it was loaded in a NuPAGE® Novex 4-12% 2D Bis-Tris gel (Invitrogen), along with 10 µl of PageRuler Protein Ladder (10-250 kDa) (Fermentas Life Sciences, Burlington, ON, Canada) into the single marker well. The inner and outer chambers of the XCell SureLock™ Mini-Cell (Invitrogen) contained NuPAGE® MES SDS running buffer (Invitrogen). The gel was

run for 45 minutes at 200 V and then transferred to nitrocellulose using the XCell II™ Blot Module (Invitrogen) for 1 hour at 30 V. To ensure that the transfer was successful, the membrane was stained with a small amount of Ponceau stain (Sigma-Aldrich). After washing off the Ponceau stain with 1x TBST, the membrane was blocked overnight in Blotto (5% dry milk powder, 0.1% Tween-20, 50 mM Tris, 150 mM NaCl). Sera were diluted 1/500 in Blotto and incubated with the membrane for 1 hour at room temperature using a multi-channel immunoblotting device (Mini Protean II Multiscreen, Bio-Rad). The membrane was washed twice with 1x TBST and once with 1x TBS for 5 minutes each, and then incubated for 1 hour at room temperature with HRP-conjugated goat anti-mouse IgG (H+L; Jackson ImmunoResearch) diluted 1/10,000 in Blotto. After washing the membrane twice with 1x TBST and once with 1x TBS for 10 minutes each, it was visualized by enhanced chemiluminescence (ECL). Immunoblots which used purified recombinant protein instead of protein lysate were performed in the same manner as above, except that 10 µg of pure protein were loaded into the 2D well.

Characterization of intratumoural CD3+ T cells in Shionogi tumours

On day 6-7 post-castration, 5 tumour-bearing DD/S mice were sacrificed and their partially regressed tumours removed, half of which was fixed in 10% formalin for histological analysis. To isolate tumour-infiltrating lymphocytes, the other tumour half was pressed with the blunt end of a 5 mm syringe through a 40-µm membrane and the resulting cell suspension was centrifuged and re-suspended in 0.5 ml of 1.0% BSA/PBS. The master mixes were prepared at a 1/400 dilution in 1.0% BSA/PBS and consisted of the following fluorochrome-conjugated antibody combinations (all antibodies were obtained from Becton, Dickinson and Company, Oakville, ON): CD3-FITC/CD4-

PE/CD8-Cy-Chrome, CD3-FITC/CD44-PE/CD4-PerCP, and CD3-FITC/CD44-PE/CD8-Cy-Chrome. Isotype matched fluorochrome-conjugated antibodies served as negative controls. In fluorescence-activated cell sorting (FACS) tubes, 50 µl of each master mix were combined with 50 µl of each cell suspension, mixed well, and then allowed to stain overnight in the dark at 4 ºC. The next day, the samples were washed with 2-3 ml of 1.0% BSA/PBS, centrifuged at 1,200 rpm for 5 minutes, and then re-suspended in 400 µl of 1.0% BSA/PBS. Each sample was run on a BD FACSCalibur^{TM} flow cytometry system (Becton, Dickinson and Company) and then the data were analyzed using FlowJo software (Tree Star, Inc., Ashland, OR).

Determining whether immune responses delay tumour recurrence in the murine Shionogi carcinoma model

Thirty-five adult male DD/S mice were injected subcutaneously with approximately 5 x 10^6 Shionogi carcinoma cells into the neck region. When the tumour reached a size between 64-100 mm^2, the mouse was castrated. Blood samples were collected from each mouse before tumour inoculation and castration, and then once per week following castration. The blood samples were centrifuged and the serum was stored at -80ºC for future use in immunoblotting assays to determine the proportion of mice with antibody responses. Tumour size (length x width) was measured using microcalipers three times per week following tumour inoculation. A tumour was considered to have recurred once it was palpable, which corresponded to ~36 mm^2. Each animal was sacrificed when its recurrent tumour reached a size approximately equal to 10% of its total body weight. At the time of sacrifice, a cardiac puncture was performed and the tumour removed, half of which was flash frozen in liquid nitrogen and the other

half submerged in 10% formalin. The spleen from each mouse was removed and pulverized into a single cell suspension using the blunt end of a 5 mm syringe and a 40-μm cell strainer. The splenocytes were re-suspended in ACK lysis buffer to lyse the red blood cells and then counted using trypan blue and a hemocytometer. The splenocytes were then either used in an IFN-γ ELISPOT assay or re-suspended in freezing media (10% DMSO/90% FBS). The entire cell suspension was aliquoted into 2 ml cryovials, which were then placed into a Mr. Frosty and frozen at -80 ºC. The next day, the tubes were transferred into a -190 ºC vapour nitrogen freezer for long-term storage.

Criteria for scoring the strength of antibody responses specific to poly(A) binding protein, nuclear 1 (PABPN1)

Immunoblots were assessed subjectively by an independent observer who was blinded to the experimental groups. The PABPN1 antibody responses were binned into three different categories, with "0" being applied to each mouse that did not exhibit a PABPN1 antibody response, "1" being assigned to each mouse that had a PABPN1 antibody response when the serum was probed against pure, recombinant PABPN1, and a "2" was assigned to each mouse that had a PABPN1 antibody response when the serum was probed against Shionogi tumour lysate, which is a less sensitive assay. A score of "2" indicated a strong antibody response based on the fact that the amount of PABPN1 present in Shionogi tumour lysate is many fold less compared to pure, recombinant PABPN1 when the antigen is detected by immunoblotting.

IFN-γ ELISPOT assay

To monitor the frequency and function of antigen-specific T cell responses, we utilized the ELISPOT assay, which is an antibody-based technique that measures

cytokine-release by activated antigen-specific T cells. We chose to measure the cytokine gamma interferon (IFN-γ) since it is secreted by both CD4+ and CD8+ T cells upon activation (9, 36). To perform the ELISPOT assay, each well of a 96-well MultiScreen$_{HTS}$ IP, 0.45 μm filter plate (Millipore, Billerica, MA) was pre-wet with 30 μl of 70% ethanol followed by three washes with 200 μl of sterile PBS. The capture antibody, 10 μg/ml anti-mouse IFN-γ AN18 (Mabtech, Mariemont, OH) diluted in sterile PBS, was added to the plate (50 μl/well) and then stored overnight at 4 ºC. The plate was washed three times with sterile PBS to remove unbound capture antibody and then the non-specific binding sites were blocked with 200 μl/well of T cell media (RPMI-1640 supplemented with 10% FBS, 1 mM sodium pyruvate, 2 mM L-glutamine, 100 μg/ml penicillin/streptomycin, and 25 μM 2-mercaptoethanol) for 2 hours at 37ºC. During this incubation, the splenocytes were prepared, counted and re-suspended in T cell media to yield a concentration of 3 x 10^6 cells/ml. The antigenic stimulus was diluted to 20 μg/ml in T cell media and concanavalin A (ConA), which was used as a positive control for the splenocytes, was diluted to 4 μg/ml in T cell medium. After the 2-hour blocking incubation, the T cell media was decanted and 100 μl of splenocytes were added to each well to give a final concentration of 3 x 10^5 cells/well. To the test wells, 100 μl of the antigenic stimulus was added to give a final concentration of 10 μg/ml, while 100 μl of ConA was added to the positive control wells to give a final concentration of 2 μg/ml. For the negative control wells, 100 μl of T cell media was added. Each sample was run in triplicate. The plate was incubated for at least 20 hours at 37 ºC. The next day, the contents of the plate were forcefully flicked out and the plate was washed six times with PBS/0.05% Tween-20. The secondary antibody, anti-mouse IFN-γ R4-6A2, biotinylated

(Mabtech), was diluted to 1 µg/ml in 0.5% BSA/PBS/0.05% Tween-20 and then 100 µl was added to each well of the plate and incubated for 2 hours at 37 ºC. Thirty minutes before the end of the incubation period, an avidin peroxidase complex (Vector Laboratories, Burlingame, CA) was prepared by adding 1 drop of reagent A plus 1 drop of reagent B to 10 ml of PBS/0.05% Tween-20 and incubated at room temperature in the dark. After the 2-hour incubation period, the plate was washed six times with PBS/0.05% Tween-20, left fully immersed in PBS/0.05% Tween-20 for 15 minutes, and then washed another six times with PBS/0.05% Tween-20. The avidin peroxidase complex (100 µl/well) was added and incubated for 1 hour at room temperature. Following the incubation period, the plate was washed six times with PBS/0.05% Tween-20, left fully immersed in PBS/0.05% Tween-20 for 15 minutes, and then washed four times with PBS. Using the Vectastain AEC substrate kit (Vector Laboratories), the developing solution was prepared by adding 4 drops of buffer stock, 6 drops of AEC substrate reagent, and 4 drops of hydrogen peroxide to 10 ml dH_2O and then 100 µl/well was added to the plate. The plate was developed for approximately 5-10 minutes, using the positive control wells as a guide for the desired exposure. Development was stopped by rinsing the plate under tap water. The air-dried plates were sent to ZellNet Consulting, Inc. (Fort Lee, NJ) for enumeration of the spots using an automated ELISPOT reader system (Carl Zeiss) with KS ELISPOT Software 4.9. Each spot corresponded to a single cytokine-producing cell (9).

Results

Castrated DD/S mice mount a treatment-associated antibody response against PABPN1 in the murine Shionogi carcinoma model

Recently, Nesslinger *et al.* (26) showed that standard treatments for prostate cancer, such as HT and EBRT, induce tumour-specific antibody responses in human prostate cancer patients. However, it is not yet known whether these treatment-induced antibody responses influence clinical outcomes since the majority of human prostate cancer patients remain tumour-free for many years following an initial course of therapy. Therefore, we set out to answer this question using a mouse model because we could determine outcomes within a much shorter time frame. Furthermore, using a mouse model allowed us to establish the time course of the immune response following treatment, as well as determine the subsets of lymphocytes that are involved in these tumour-specific immune responses. We hypothesized that in the murine Shionogi carcinoma model, castrated DD/S mice that mount treatment-associated tumour-specific immune responses will have delayed tumour recurrence and prolonged survival relative to those mice that do not mount treatment-associated tumour-specific immune responses.

In preliminary experiments using the murine Shionogi carcinoma model, we previously showed that approximately 50% of castrated DD/S mice mounted an IgG antibody response against a ~40 kDa antigen (26). Since this was the most common treatment-associated antibody response observed, we hypothesized that it was likely accompanied by a T cell response to the ~40 kDa antigen due to the fact that the CD4+ T helper response is essential for the development and fine tuning of antibody responses with respect to the quality of antibody produced (i.e. affinity) and the expression of

particular idiotypic determinants on the secreted antibody molecules (37). In order to determine whether castration also induces a T cell response against the ~40 kDa antigen, it would be most convenient to use pure antigen for stimulating the T cells in an immunoassay. To obtain pure antigen we needed to identify and then clone the ~40 kDa antigen. One approach that we considered to identify the ~40 kDa antigen was the T cell epitope cloning method developed by Boon and colleagues (38). However, this approach is complex, laborious and time-consuming due to the difficulty associated with establishing stable T cell lines and tumour lines. Conversely, defining antibody targets is far less complex than T cell cloning methods and the analysis of humoral immunity to tumour antigens has the potential for identifying antigens recognized by both CD4+ T helper cells and CD8+ cytotoxic T cells (39, 40). Therefore, we decided to utilize SEREX screening since it is a widely used, relatively easy and fast approach for identifying antibody targets. Furthermore, our laboratory had the resources, including an abundance of serum from the preliminary experiment that was positive for the ~40 kDa antigen, and expertise to successfully employ this technique. For convenience and efficiency, we determined if the ~40 kDa antigen had a human homolog since we already had a phage cDNA expression library made from human prostate cancer cell lines. Using serum from castrated DD/S mice to probe protein lysate from a human prostate cancer cell line, LNCaP, we showed that the ~40 kDa antigen does indeed have a human homolog (Figure 1). Therefore, screening the human prostate cancer phage cDNA expression library with serum positive for the ~40 kDa antigen was performed to clone the ~40 kDa antigen.

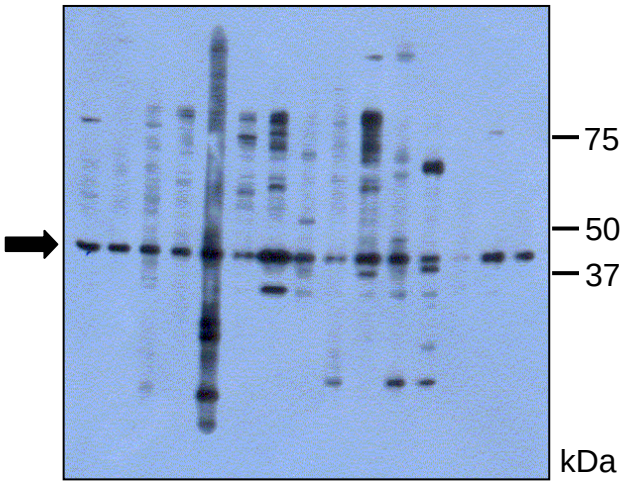

Figure 1. The ~40 kDa antigen identified in Shionogi tumour lysate has a human homolog. LNCaP protein lysate was screened with fifteen different serum samples obtained from the terminal bleeds of castrated DD/S mice. The arrow indicates the ~40 kDa antigen of interest.

Briefly, SEREX immunoscreening involved infecting bacterial cells with an aliquot of the prostate cancer phage cDNA expression library and then plating them on NZYCM agar, where the presence of colonies indicated bacterial growth and lysis and hence, protein expression. The proteins were captured on an IPTG-soaked nitrocellulose membrane, which was then screened with Shionogi serum that was positive for the ~40 kDa antigen as determined by immunoblotting (see Figure 1). An anti-mouse IgG secondary antibody was used to detect membrane-bound anti-Shionogi tumour antibodies. Membrane development showed antigens of interest as dark purple spots, which were cored and re-screened to confirm their positivity. SEREX immunoscreening of approximately 1.6×10^4 clones yielded four positive antigens, which were all confirmed as positive through secondary screening. The positive phagemids were converted into plasmids, which were then sequenced and identified using NCBI Blast. The four positive antigens identified by SEREX immunoscreening corresponded to four different gene products. SH3-domain GRB2-like endophilin B1 (SH3GLB1) is a 40 kDa protein that is an important component of many signalling pathways (41). Crooked neck-like 1 (CRNKL1) is an 83 kDa protein that has been implicated in cell cycle progression and in pre-mRNA splicing, while malate dehydrogenase (MDH) is a 37 kDa protein that catalyzes the interconversion of oxaloacetate and malate in the tricarboxylic acid cycle (42, 43). Finally, PABPN1 is a 33 kDa protein that is required for the efficient polymerization of poly(A) tails on the 3' ends of eukaryotic mRNAs (44). The mouse version of each of the identified antigens was cloned from Shionogi tumour cells using Invitrogen's Gateway system, and *E. coli* His-tagged recombinant protein was produced and purified. Immunoblotting using serum that was known to be positive or negative for

the ~40 kDa antigen revealed that *E. coli* recombinant SH3GLB1, CRNKL1, and MDH were not recognized by any of the mouse sera (Figure 2A). A possible explanation for why SH3GLB1, CRNKL1, and MDH were positive by SEREX but negative by immunoblotting may be due to differences in the reading frame used by *E. coli* transfected phage compared to the *E. coli* recombinantly expressed protein. For example, Invitrogen's Gateway cloning system ensured that each of the *E. coli* recombinant antigens was expressed in the proper reading frame, whereas the antigens encoded by the *E. coli* transfected phage may have been translated in any one of a possible six reading frames. Irrespective of the precise reason, these gene products clearly did not represent the ~40 kDa antigen and therefore were not further evaluated.

In contrast, recombinant PABPN1 was recognized by those mouse sera that were seroreactive to the ~40 kDa antigen (Figure 2B). We were further convinced that PABPN1 was the ~40 kDa antigen by the observation that mouse sera that were not seroreactive to the ~40 kDa antigen were, for the most part, also not seroreactive to recombinant PABPN1. Some of the serum samples that were negative for the ~40 kDa antigen when probed against Shionogi tumour lysate appeared weakly positive when probed against recombinant PABPN1, as shown in the immunoblot in Figure 2B. However, this could be attributed to the difference in the amount of PABPN1 present in an immunoblot containing Shionogi tumour lysate, which is many fold less, compared to the amount of PABPN1 present in an immunoblot containing recombinant PABPN1. Therefore, probing against recombinant PABPN1 is more sensitive for detecting PABPN1 antibody responses than probing against Shionogi tumour lysate. In summary,

the pattern of seroreactivity to PABPN1 was entirely consistent with it being the ~40 kDa antigen.

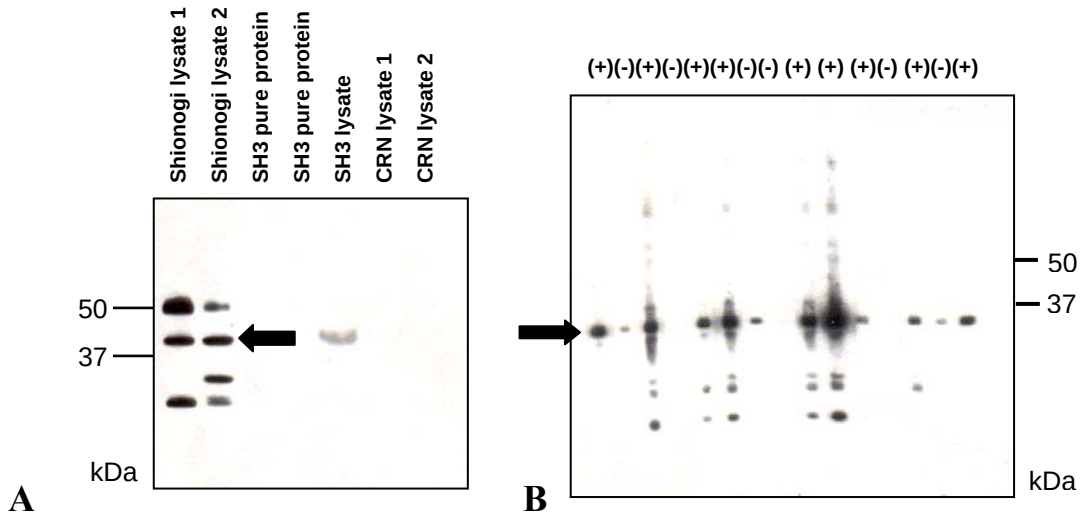

Figure 2. Recombinant SH3GLB1 and CRNKL1 are not recognized by mouse sera that is seroreactive for the ~40 kDa antigen, whereas recombinant PABPN1 is recognized by sera that is seroreactive for the ~40 kDa antigen, and in most instances, is not recognized by sera that is not seroreactive for the ~40 kDa antigen. *A*, Shionogi tumour lysate (20 µg), SH3GLB1 pure protein (20 µg), SH3GLB1 *E.coli* lysate (100 µg), and CRNKL1 *E.coli* lysate (100 µg) were screened with serum positive for the ~40 kDa antigen. The ~40 kDa antigen appears in the lanes containing Shionogi tumour lysate (arrow), but not in the lanes containing recombinant SH3GLB1 and CRNKL1. The faint band in the lane containing SH3GLB1 lysate is not a real positive, rather background ECL staining due to the large amount of protein present. In the lanes containing Shionogi lysate1 and Shionogi lysate2, the seroreactive bands appearing at ~55 kDa and ~25 kDa correspond to the IgG heavy and light chains, respectively. These bands appear as a result of the secondary goat anti-mouse IgG antibody reacting with IgG present in the Shionogi tumour lysate preparations. *B*, purified, soluble, recombinant PABPN1 (10 µg) was screened with serum that was known to be positive (+) or negative (-) for the ~40 kDa antigen. The correlation between expected positives and negatives was high; however, some negatives did appear faintly positive.

One issue concerned the difference in molecular weight between the ~40 kDa antigen identified in Shionogi tumour lysate and recombinant PABPN1, which is 33 kDa (see Figure 2B). We reasoned that PABPN1 may undergo post-translational modifications when expressed by Shionogi cells, resulting in a higher molecular weight. Indeed, it has also been reported that PABPN1 migrates in SDS-polyacrylyamide gels at ~49 kDa (45). We investigated this notion in our tumour model using an immunization strategy, whereby we immunized 5 male naïve DD/S mice subcutaneously with 100 µg of recombinant PABPN1 in incomplete Freund's adjuvant (IFA) and then 2 weeks later gave them one booster immunization. Blood samples from each mouse were collected one week following the boost, and the sera were used to probe Shionogi tumour lysate and recombinant PABPN1. The presence of an immunoreactive band at ~40 kDa on the membrane containing Shionogi tumour lysate reaffirmed that the ~40 kDa antigen we set out to identify was indeed PABPN1 despite the difference in molecular weight of the recombinant form (Figure 3). As speculated, post-translational modifications to PABPN1 in Shionogi tumour cells may explain why it appears at ~40 kDa on immunoblots containing Shionogi tumour lysate compared to its calculated molecular weight of 33 kDa. Further confirmation of this hypothesis could be tested by expressing recombinant PABPN1 in mammalian cells rather than bacterial cells.

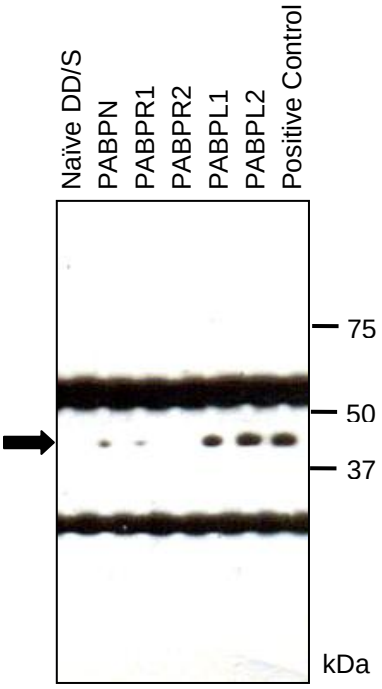

Figure 3. PABPN1 is the ~40 kDa antigen recognized by serum antibodies from castrated mice. Shionogi tumour lysate was screened with serum from a naïve DD/S mouse and 5 mice (PABPN, PABPR1, PABPR2, PABPL1, PABPL2) that were each immunized twice with 100 µg of PABPN1 in IFA 2 weeks apart. The presence of an immunoreactive band at ~40 kDa (arrow) confirms that PABPN1 is the ~40 kDa antigen. The positive control consisted of serum that was known to be seroreactive for the ~40 kDa antigen. The continuous seroreactive bands on the blot at ~55 kDa and ~25 kDa correspond to the IgG heavy and light chains, respectively.

We were interested in why PABPN1, an ubiquitously expressed self-protein, was being recognized by the immune system in tumour-bearing DD/S mice following castration. We speculated that PABPN1 may be over-expressed in Shionogi tumours. To determine this, we examined the expression of PABPN1 in a variety of normal mouse tissues relative to the level of expression in Shionogi tumour lysate (Figure 4).

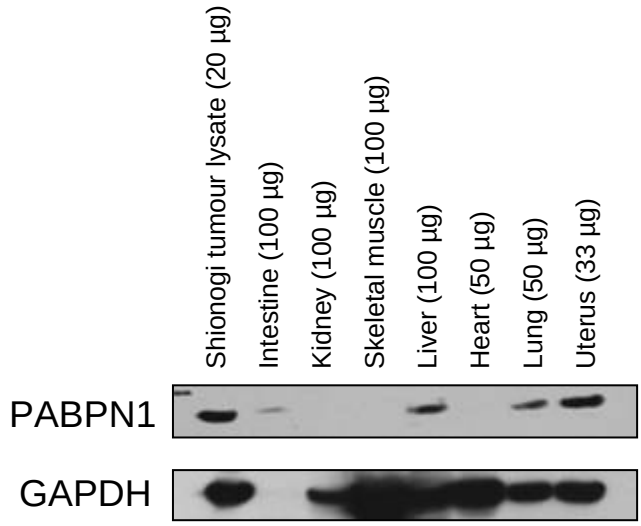

Figure 4. PABPN1 is expressed in Shionogi tumour lysate, as well as normal intestinal, liver, lung, and uterine tissues. For each normal tissue, as much protein as possible was loaded per lane. Serum from one of the PABPN1-immunized mice (PABPL2) was used as the primary antibody. GAPDH served as a loading control.

The immunoblot in Figure 4 shows that PABPN1 is expressed at high levels in Shionogi tumour lysate, as well as normal liver, lung and uterine tissues. By contrast, PABPN1 is expressed at low levels in normal intestinal, kidney, skeletal muscle, and heart tissues. This finding is in accordance with a previously published study in which 12 normal human tissues were analyzed by Affymetrix for PABPN1 expression. In this study, PABPN1 was expressed at lower levels in normal kidney, muscle, and heart tissues compared to intestinal, liver, lung, and uterine tissues (46, GeneNote Version 2.1). Although there is a discrepancy between the immunoblot in Figure 4 and the published data with respect to PABPN1 expression in normal intestinal tissues, it can be attributed to the poor quality of the intestinal protein lysate, as indicated by the absence of GAPDH in this sample. Although PABPN1 has not been shown to be overexpressed in cancer, the fact that it plays a functional role in several transcriptional processes may be a reason for its high level of expression in Shionogi tumour cells (44). The observation that PABPN1 is expressed at high levels in several normal tissues raises the issue of why it becomes immunogenic only after castration of tumour-bearing mice. We speculate that immunological tolerance to this self-antigen is broken, not due to over-expression, but rather due to some inflammatory event that occurs during the process of tumour regression.

Timing and frequency of antibody responses to PABPN1 in castrated tumour-bearing DD/S mice

To establish the time course of the immune response in the murine Shionogi carcinoma model, groups of 8-10 male, tumour-bearing DD/S mice were sacrificed at five specific time points following castration, while animals in a “no treatment” control

group consisting of 10 male, tumour-bearing DD/S mice were not castrated. As before, all of the tumours partially or completely regressed following castration, and of those mice sacrificed at later time points, the large majority experienced tumour recurrence (Figure 5).

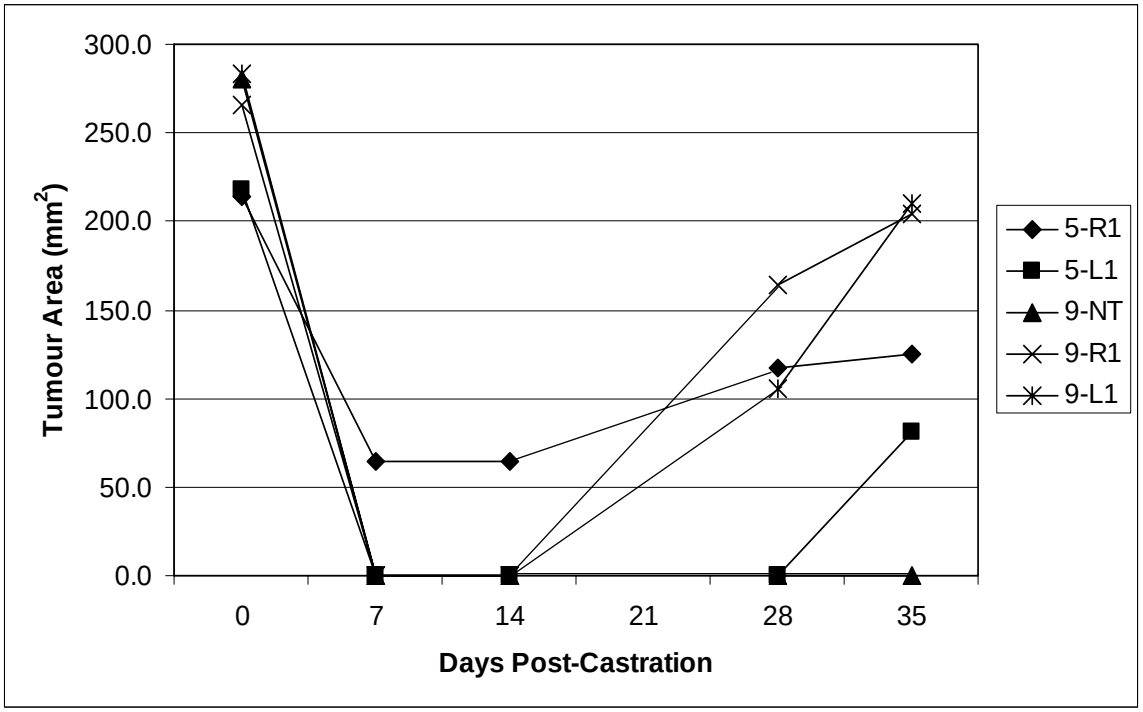

Figure 5. Representative graph of tumour area versus days post-castration for 5 mice that were sacrificed on day 35 post-castration. Following castration on day 0, 4 of the 5 mice had complete tumour regression, while 1 mouse had partial tumour regression. The tumours recurred between 14-28 days post-castration. The legend corresponds to the individual mouse IDs.

Pre-tumour, pre-castration, and terminal serum samples from this cohort of mice were probed against recombinant PABPN1, which allows detection of even low level antibody responses (Figure 2B). As before, none of the tumour-bearing, non-castrated mice showed an antibody response against PABPN1. Antibody responses against PABPN1 were detectable as early as day 7 post-castration, with 88% (7/8) of mice sacrificed at this time point showing a faint seroreactive band by immunoblotting. Antibody responses got progressively stronger and peaked in magnitude and prevalence by day 28 post-castration, and were maintained at this level at later time points. Overall, 65% (31/48) of castrated mice showed a treatment-associated antibody response against PABPN1 (Figure 6).

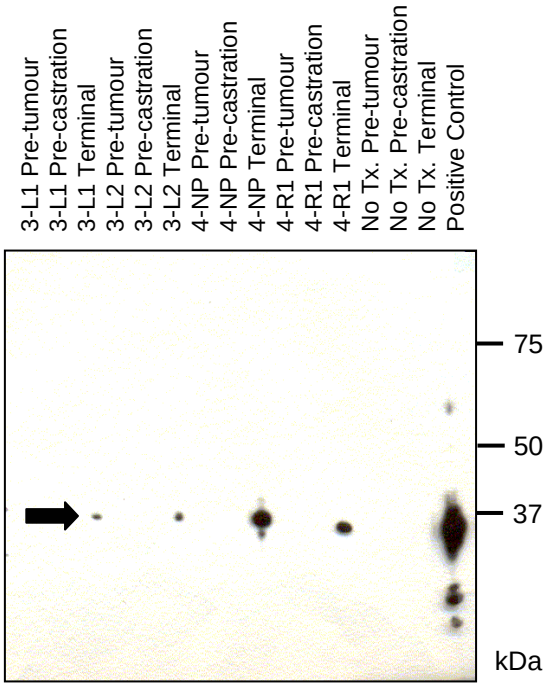

Figure 6. Castration induced an antibody response against PABPN1 in a large proportion of mice. Purified, soluble, *E. coli* recombinant PABPN1 (10 µg) was probed with pre-tumour, pre-castration, and terminal serum samples obtained from castrated mice 3-L1, 3-L2, 4-NP, 4-R1, and a tumour-bearing, non-castrated (No Tx.) mouse. 3-L1 and 3-L2 were sacrificed on day 28 post-castration and 4-NP and 4-R1 were sacrificed on day 33 post-castration. The arrow shows the PABPN1 seroreactive band. The positive control consisted of serum that was known to be seroreactive for the ~40 kDa antigen.

As per our published study, we also probed sera against Shionogi tumour lysate to see if other antigens, aside from PABPN1, were recognized by the immune system of castrated DD/S mice. For this analysis, we used all of the serum samples obtained from each mouse to precisely define the time course of antibody development. As expected, no antibody responses were observed in tumour-bearing, non-castrated mice, or in the pre-tumour and pre-castration serum samples from the castrated mice. In contrast, 33% (16/48) of castrated mice mounted an antibody response against one or more Shionogi tumour antigens, with an average time of approximately 21 days post-castration to develop the antibody response (Figure 7). In the vast majority (14/16) of these cases, the antibody response was to the ~40 kDa antigen, corresponding to PABPN1. Castration also induced an antibody response against a ~60 kDa antigen in 4 mice, and antigens of ~25, ~30, and ~35 kDa in one mouse each. As PABPN1 was by far the most commonly recognized antigen, we did not determine the identity of any of these other antigens.

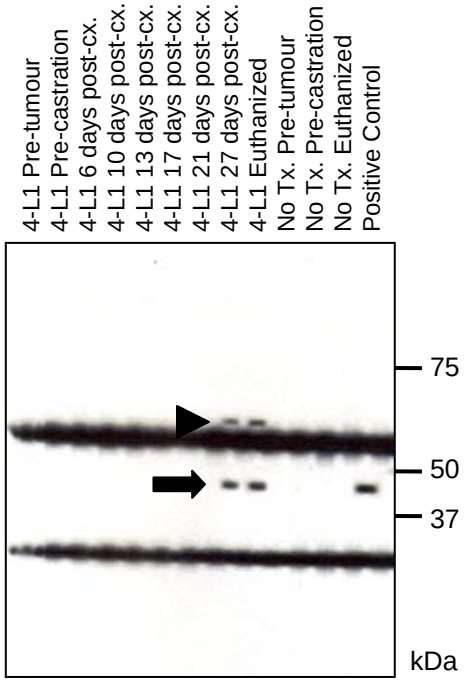

Figure 7. Castration induced antibody responses against PABPN1 and other Shionogi tumour-specific antigens. Shionogi tumour lysate was probed with serum samples from mouse 4-L1 (sacrificed 33 days post-castration) and a non-castrated (No Tx.) mouse. An antibody response against PABPN1 (arrow) and a larger tumour antigen (~60 kDa, arrowhead) appeared at day 27 post-castration, while no antibody response was observed in the non-castrated mouse. The positive control consisted of serum that was known to be seroreactive for the ~40 kDa antigen. The continuous seroreactive bands on the blot at ~55 kDa and ~25 kDa correspond to the IgG heavy and light chains, respectively.

Shionogi tumours become densely infiltrated by CD3+ T cells 7-14 days post-castration

Following castration, Shionogi tumour cells undergo massive apoptosis due to the loss of androgens on which they depend for growth and viability (32). Tumour cell apoptosis likely releases antigen into the tumour microenvironment, which could potentially be taken up by professional APCs, which in turn may prime antigen-specific T cell responses in draining lymph nodes. Such T cell responses typically result in migration and infiltration of T cells to the tumour bed (21, 47). To see whether Shionogi tumours become infiltrated by T cells after castration, we constructed a tissue microarray from the formalin-fixed Shionogi tumours and stained them for the T cell marker CD3 by immunohistochemistry (IHC). Anti-CD3 staining revealed that primary tumours from non-castrated mice had very few CD3+ T cells present within the tumour and in the surrounding stroma, therefore baseline T cell responses appear to be minimal in this model. In contrast, all of the tumours were densely infiltrated with CD3+ T cells between 7-14 days post-castration (Figure 8, 9). When the tumour-infiltrating CD3+ T cells were further examined by FACS on days 6-7 post-castration, approximately 55% were CD8+ T cells and 24% were CD4+ T cells (averaged over three independent experiments) (Figure 10). Interestingly, over 95% of the CD4+ and CD8+ T cells were activated as determined by staining for the T cell activation marker CD44.

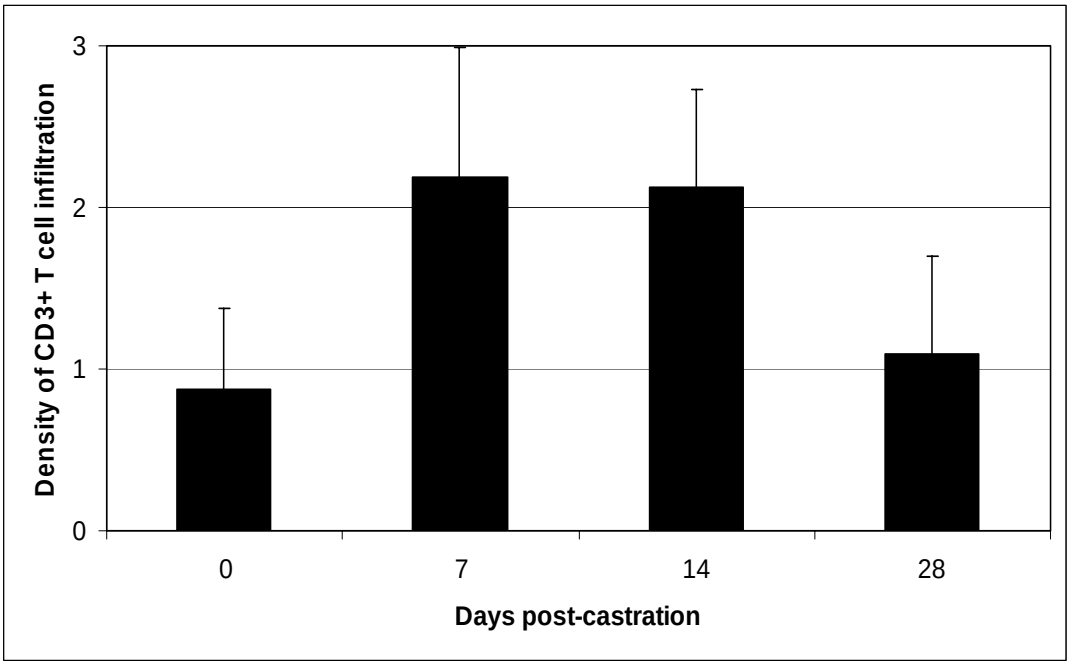

Figure 8. Anti-CD3 staining revealed that Shionogi tumours from non-castrated mice (day 0) contained very low numbers of CD3+ T cells compared to tumours from castrated mice sacrificed on days 7 and 14 post-castration, which were densely infiltrated with CD3+ T cells.

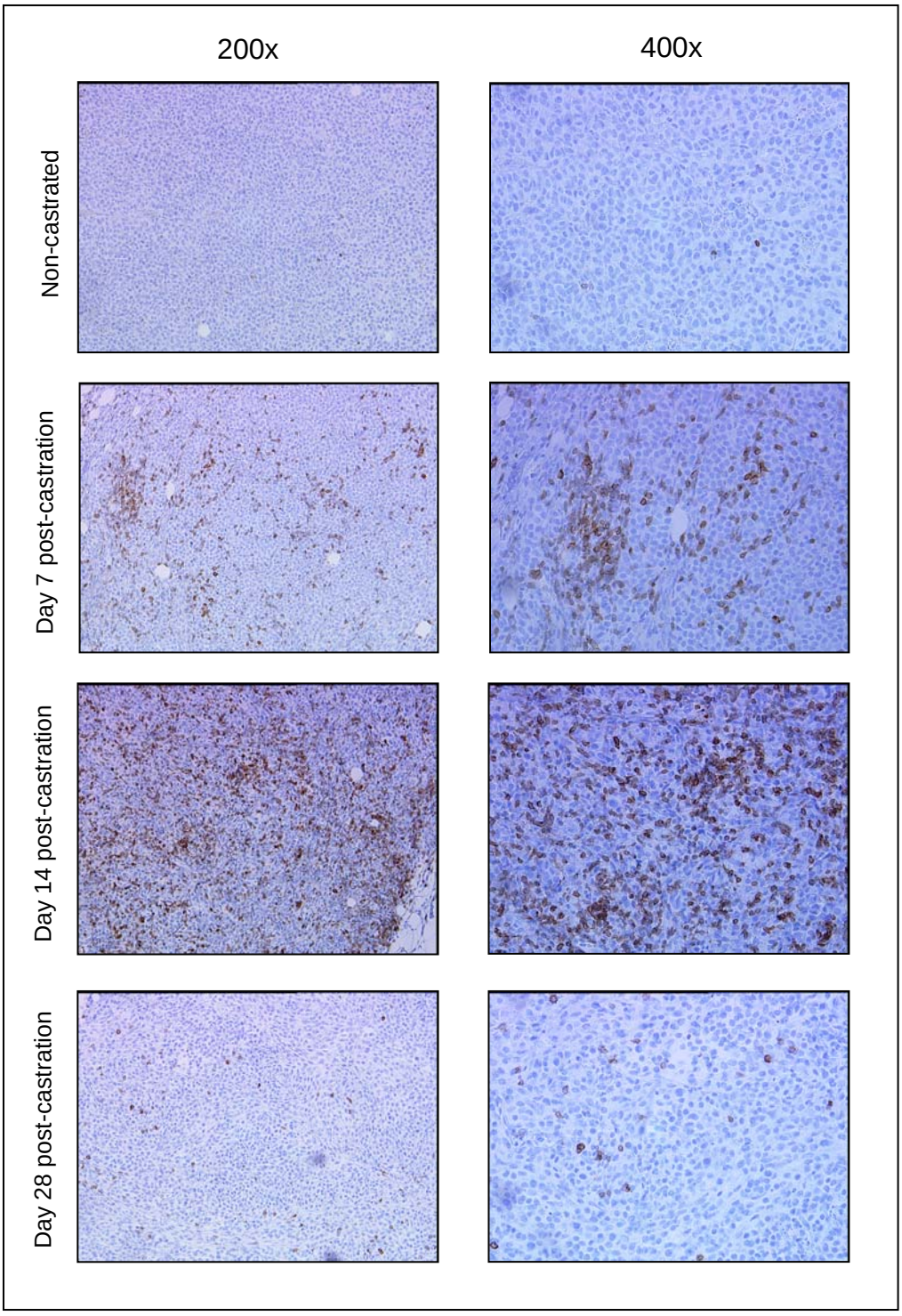

Figure 9. Anti-CD3 staining of Shionogi tumours at specific time points following castration showed dense infiltration of CD3+ T cells between 7-14 days post-castration. By 28 days post-castration, when most of the tumours had recurred, CD3+ T cells were sparse. The tumours from non-castrated mice were essentially devoid of CD3+ T cells.

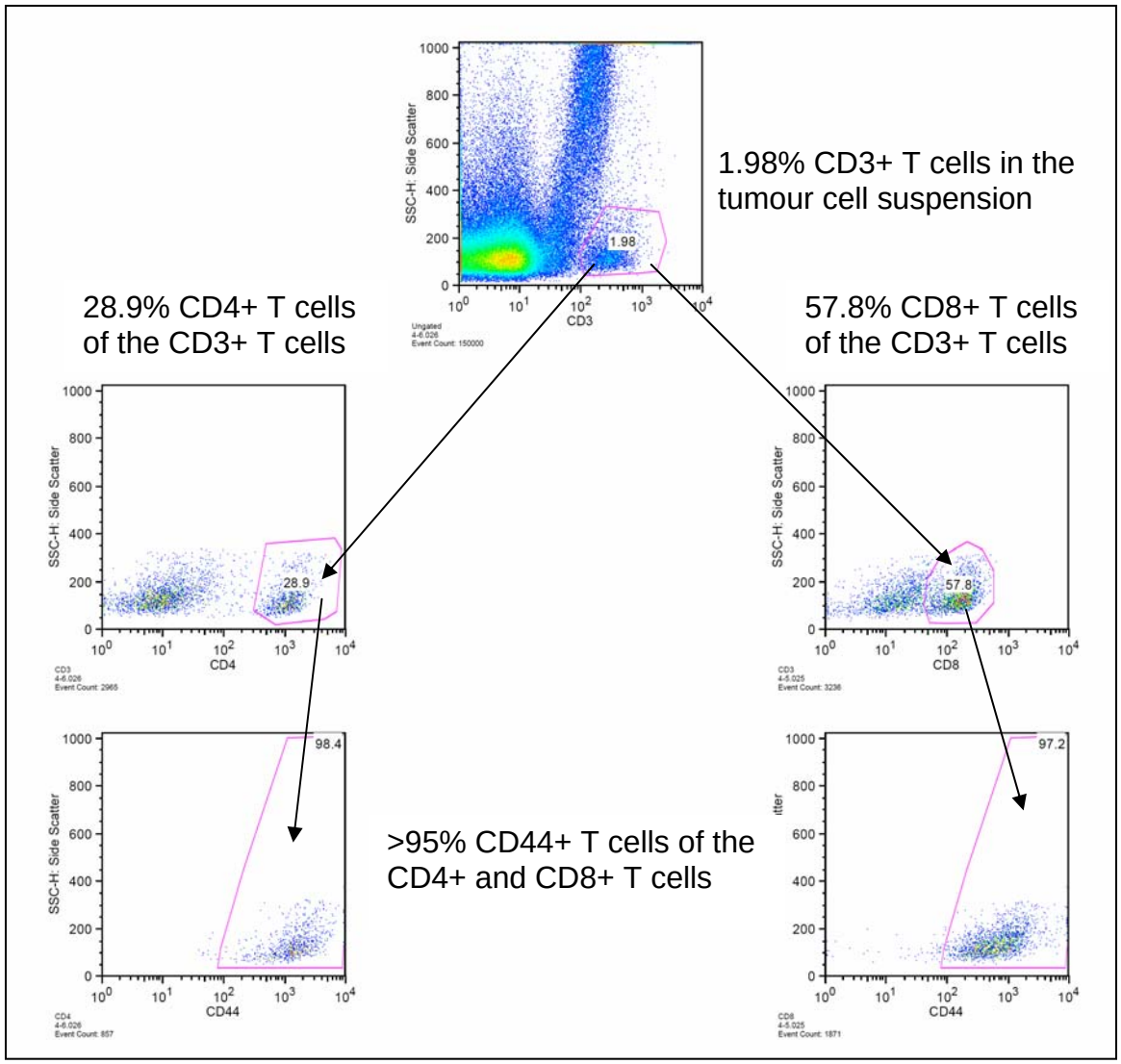

Figure 10. Representative FACS plots showing that the vast majority of the CD4+ and CD8+ T cells within a tumour on day 7 post-castration are activated as determined by CD44 expression.

We next examined T cell infiltrates for evidence of cytolytic effector function. The tissue microarray was stained with an antibody for granzyme B, a serine protease that is a component of cytolytic granules in cytotoxic CD8+ T cells and natural killer (NK) cells (Figure 11) (48). Anti-granzyme B staining of Shionogi tumours revealed no granzyme B positive cells, despite the fact that adjacent sections showed dense CD3+ T cell infiltrates that were CD44+ by FACS (see Figure 10). This implies that the infiltrating T cells lacked granzyme B-mediated cytolytic function on days 7 and 14 post-castration (see Figure 9).

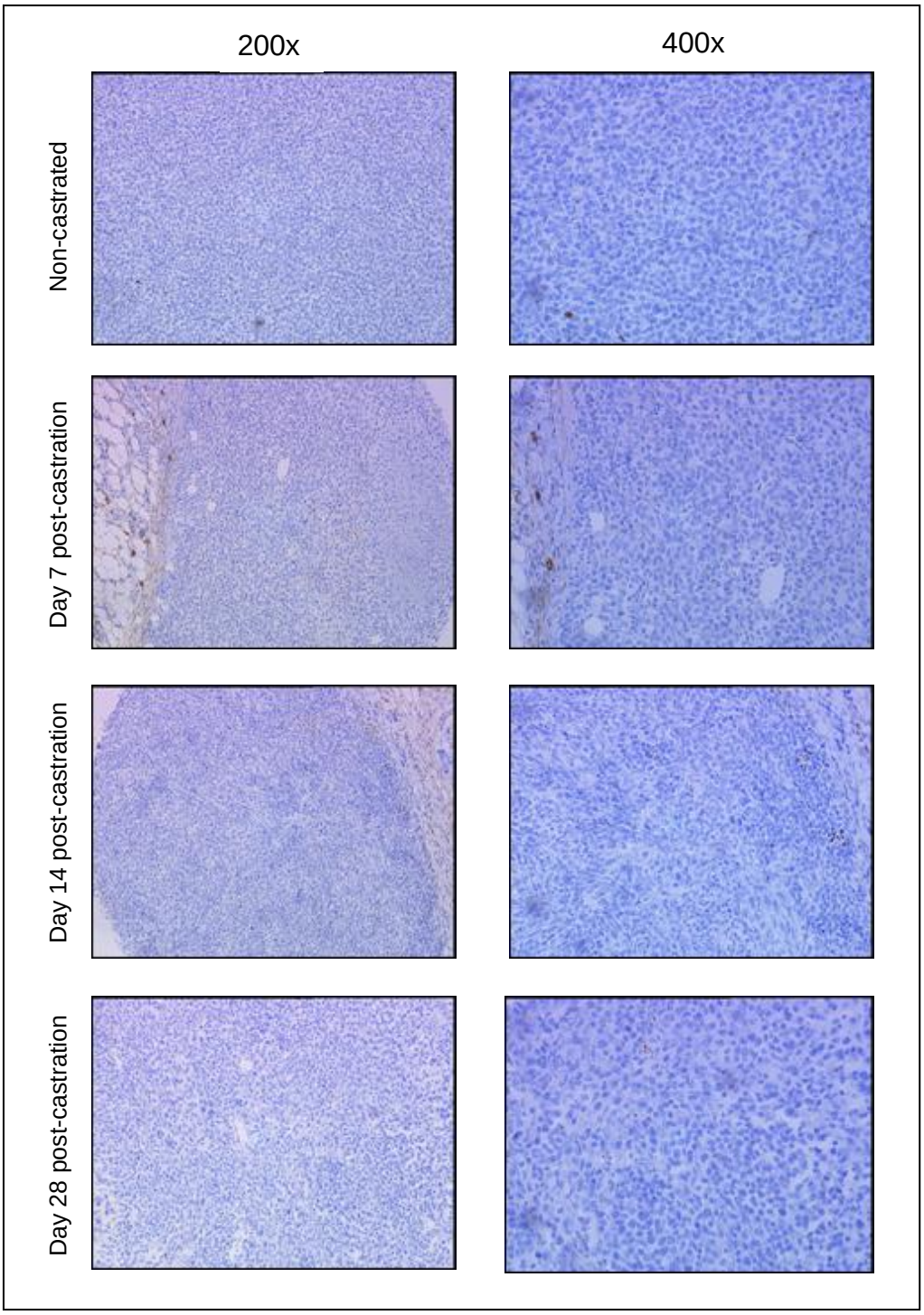

Figure 11. Anti-granzyme B staining of Shionogi tumours at specific time points following castration revealed that the vast majority of infiltrating CD3+ T cells lacked granzyme B-mediated cytolytic function.

Regulatory T cells (Tregs) mediate peripheral tolerance by suppressing autoreactive T cells, but they have also been implicated in the suppression of tumour-specific T cell immunity, thus contributing to tumour growth. We stained the Shionogi tumours for FoxP3, a transcription factor gene product unique to Tregs (49). In general, the percentage of intratumoural FoxP3+ Tregs correlated with the proportion of intratumoural CD3+ T cells, such that tumours that were densely infiltrated with CD3+ T cells appeared to have the most Tregs (~5-10% of the CD3+ T cells), while tumours that contained very few CD3+ T cells contained very few Tregs (Figure 12). Accordingly, the number of Tregs found in tumours from non-castrated mice was negligible. Thus, the presence of intratumoural Tregs raises the possibility that these suppressive T cells may play a role in dampening tumour-specific immune responses induced by castration in this mouse model.

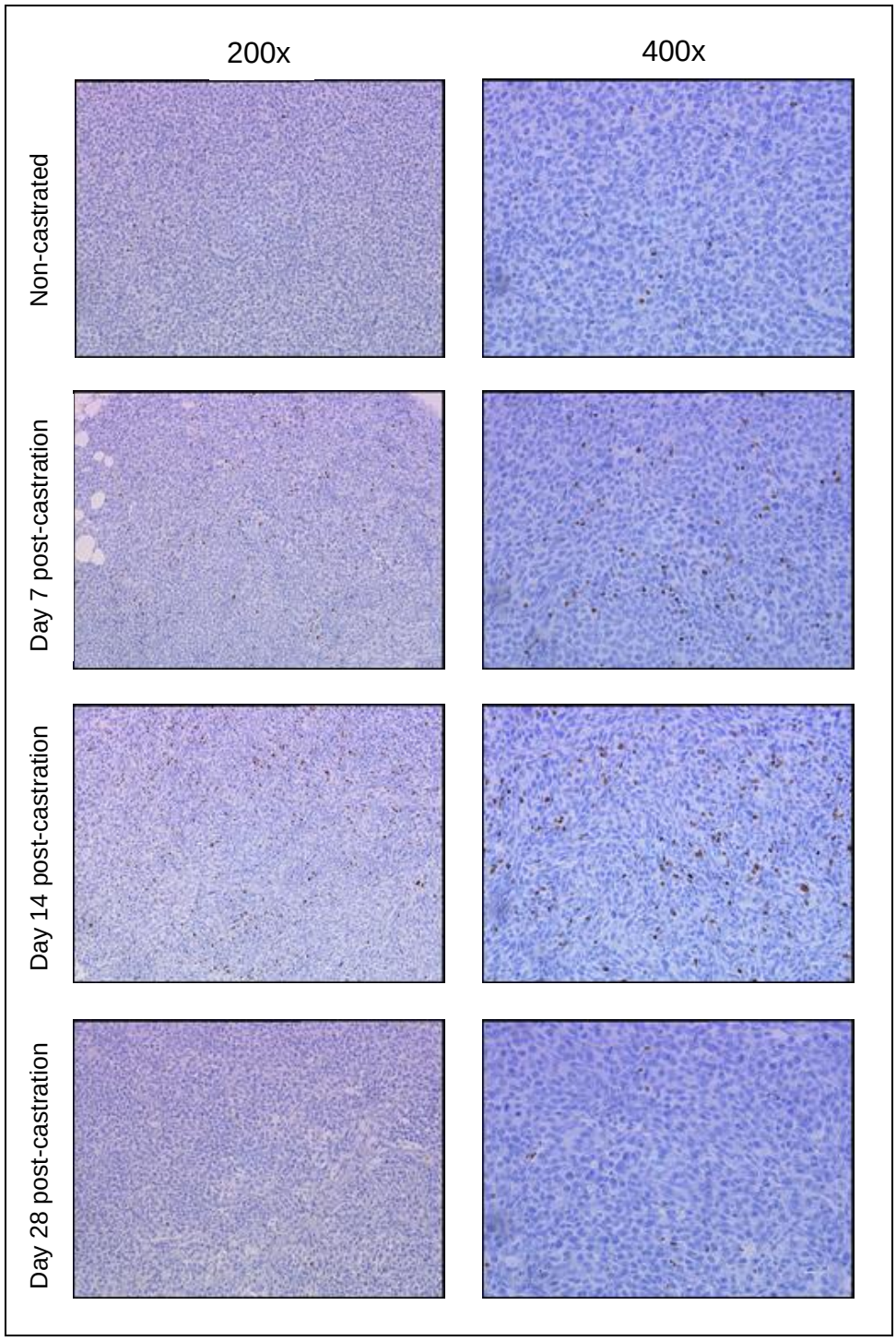

Figure 12. Anti-FoxP3 staining of Shionogi tumours at specific time points following castration revealed that the proportion of Tregs present within the tumours was highest on days 7 and 14 post-castration, which is also when the tumours were densely infiltrated with CD3+ T cells.

We also stained our tissue microarray with an antibody for a B cell transcription factor, Pax-5 (50). Despite the robust antibody responses to PABPN1 in many mice, the number of B cells found within the Shionogi tumours was negligible (Figure 13). Therefore, we assume that the B cells making the antibodies are found within the bone marrow or secondary lymphoid organs.

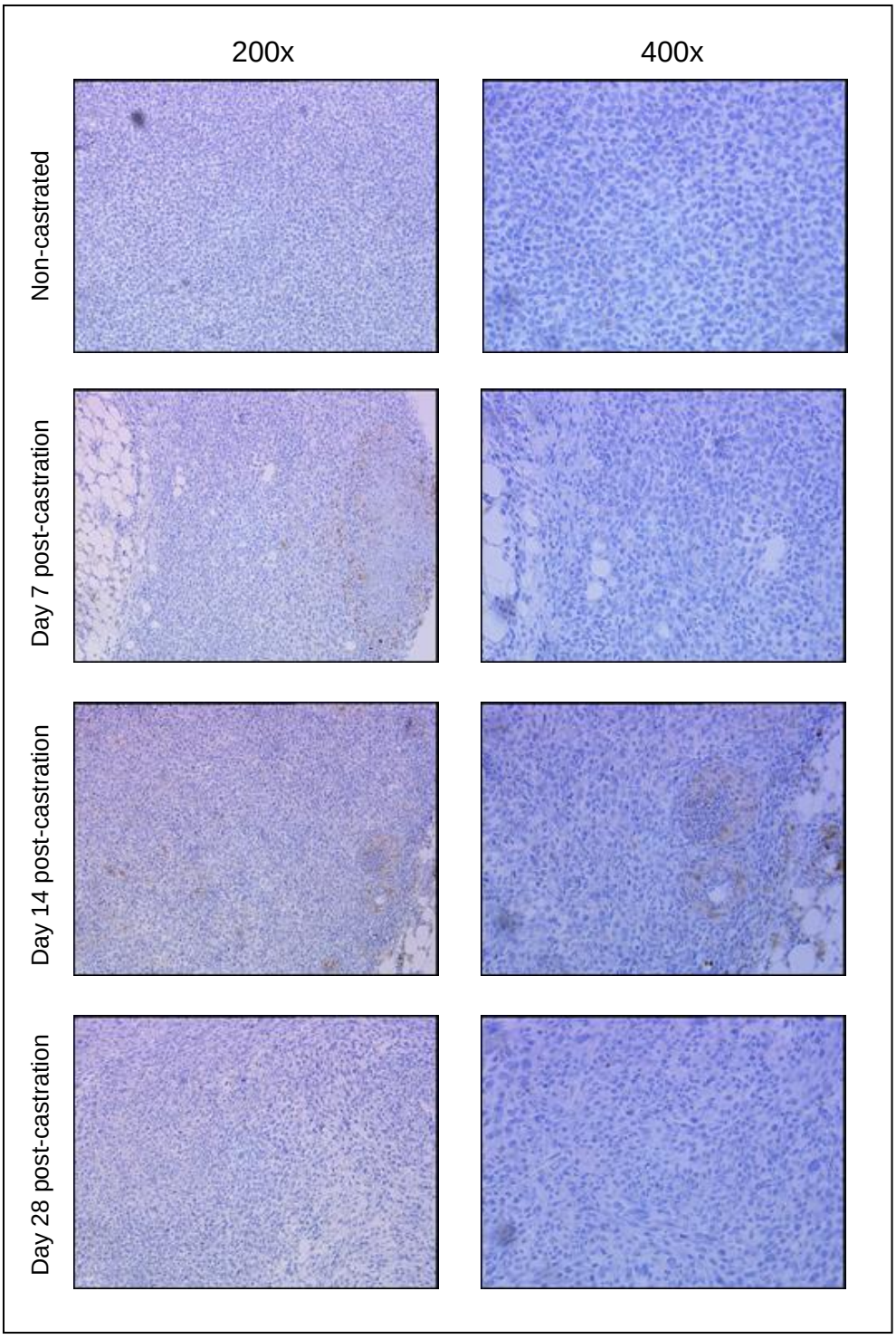

Figure 13. Anti-Pax-5 staining of Shionogi tumours at specific time points following castration revealed that very few B cells were present within the tumours. The faint brown staining in some of the images above corresponds to non-specific background staining.

Beyond 14 days post-castration, CD3+ T cell infiltrates became progressively more sparse, which coincided with tumour recurrence. Anti-FoxP3 staining showed that the number of Tregs within the tumours diminished as the number of CD3+ T cells decreased. The sporadic CD3+ T cells present within the recurrent tumours lacked granzyme B-mediated cytolytic function, as shown by the absence of granzyme B positive cells. Like the primary tumours, the recurrent tumours did also not become infiltrated by B cells. Microscopic observation of the H&E-stained recurrent Shionogi tumours revealed that they were generally viable with a solid histological appearance around the periphery and necrotic centres.

In summary, Shionogi tumours became densely infiltrated by CD3+ T cells within 7-14 days following castration. Meanwhile, the PABPN1 antibody response was detectable by day 7 post-castration and peaked at day 28. Therefore, the time course observed in this experiment represents a typical immune response in which the T cell response precedes the antibody response, likely reflecting the need for CD4+ T helper responses to promote mature IgG antibody responses.

Castration induces a T cell response against PABPN1

We speculated that the treatment-associated antibody response we observed against PABPN1 was accompanied by a T cell response to PABPN1 due to the fact that CD4+ T helper responses are essential for the development and fine tuning of antibody responses (37). To determine whether castration also induces a T cell response against PABPN1, we performed IFN-γ ELISPOT assays with splenocytes harvested from castrated, tumour-bearing mice. As a negative control for our assay, we included splenocytes from wild-type, tumour-free DD/S mice. As a positive control for our assay,

we included splenocytes from wild-type DD/S mice that were immunized subcutaneously with 200 μg PABPN1 + 100 μg polyinosinic:polycytidylic acid (poly I:C) and then sacrificed 7 days later when the T cell response was expected to be at a maximum. As expected, wild-type DD/S mice immunized with PABPN1 + poly I:C showed a moderately strong T cell response against PABPN1, whereas wild-type, tumour-free DD/S mice showed no T cell response (i.e. the number of IFN-γ spot-forming cells was similar to the number of background spots) (Figure14). As hypothesized, castrated, tumour-bearing mice showed a strong T cell response to PABPN1. We asked whether this was due to the tumour, castration or both. A non-castrated, tumour-bearing mouse showed a weak T cell response against PABPN1 (i.e. the number of IFN-γ spot-forming cells was slightly higher than the number of background spots). However, a castrated, non-tumour bearing wild-type mouse showed a moderately strong T cell response against PABPN1. This observation coincides with observations found by Roden *et al.* (51), whereby androgen deprivation in tumour-free male mice increased the absolute number of T cells residing in peripheral lymphoid tissues. One possible explanation for why a T cell response was induced following castration in the absence of a Shionogi tumour is that an inflammatory response was generated at the surgical site. An alternative explanation is that other tissues that may rely on androgens for growth, such as the prostate, undergo atrophy as a result of androgen withdrawal and consequently, an immune response is generated. Overall, castration induces a T cell response against PABPN1 and this response is exaggerated in tumour-bearing mice. In contrast, as described before, antibody responses to PABPN1 are only seen upon castration of tumour-bearing mice.

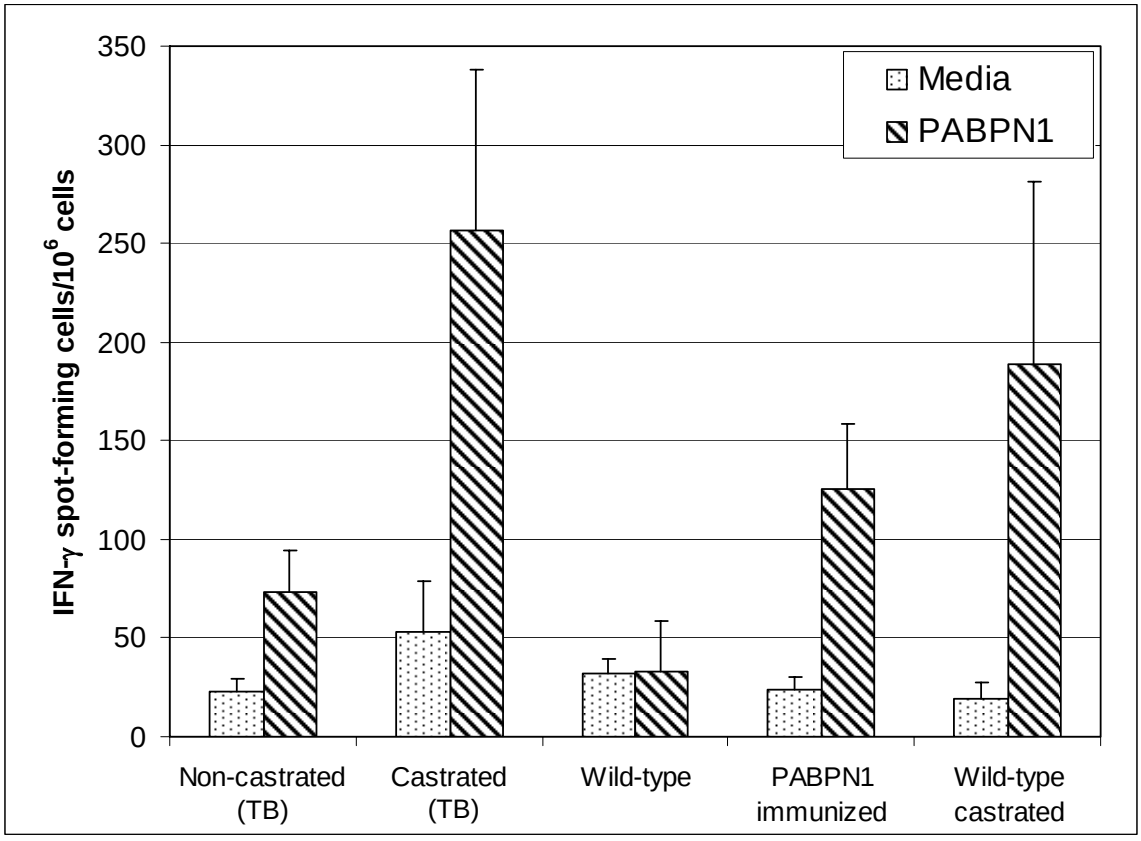

Figure 14. Castration induces a PABPN1-specific T cell response in both tumour-bearing (TB) and non-tumour bearing wild-type DD/S mice, as measured by IFN-γ ELISPOT. For the non-castrated, castrated and wild-type data shown on the graph, previously frozen splenocytes were used in the ELISPOT assay, while for the PABPN1 immunized and wild-type castrated data, fresh splenocytes were used in the ELISPOT assay. Each sample was run in triplicate, with the values for each well being averaged and the standard deviation calculated.

PABPN1 antibody and T cell responses are associated with early tumour recurrence

Having established the time course of the immune response following castration of tumour-bearing DD/S mice in the murine Shionogi carcinoma model, we wanted to determine if antibody and/or T cell responses against PABPN1 delay the time to tumour recurrence and prolong survival. In this experiment, 33 tumour-bearing DD/S mice were castrated when the tumour area reached 64-100 mm^2. Following castration, 32/33 mice experienced complete tumour regression, while the remaining mouse experienced partial tumour regression. Of the 32 mice that underwent complete regression, 72% (23/32) experienced tumour recurrence 3-70 days post-castration, while the remaining 28% (9/32) remained tumour-free for the duration of the experiment until they were sacrificed for analysis (64-86 days post-castration). Immunoblotting with serum samples obtained from weekly blood draws showed that 71% (17/24) of mice with recurrent tumours had an antibody response against PABPN1, whereas only 11% (1/9) of mice that remained tumour-free had a PABPN1 antibody response. Put another way, the mean tumour-free interval for those mice that had a PABPN1 antibody response was approximately 25 days compared to approximately 63 days for those mice that did not have a PABPN1 antibody response (Figure 15).

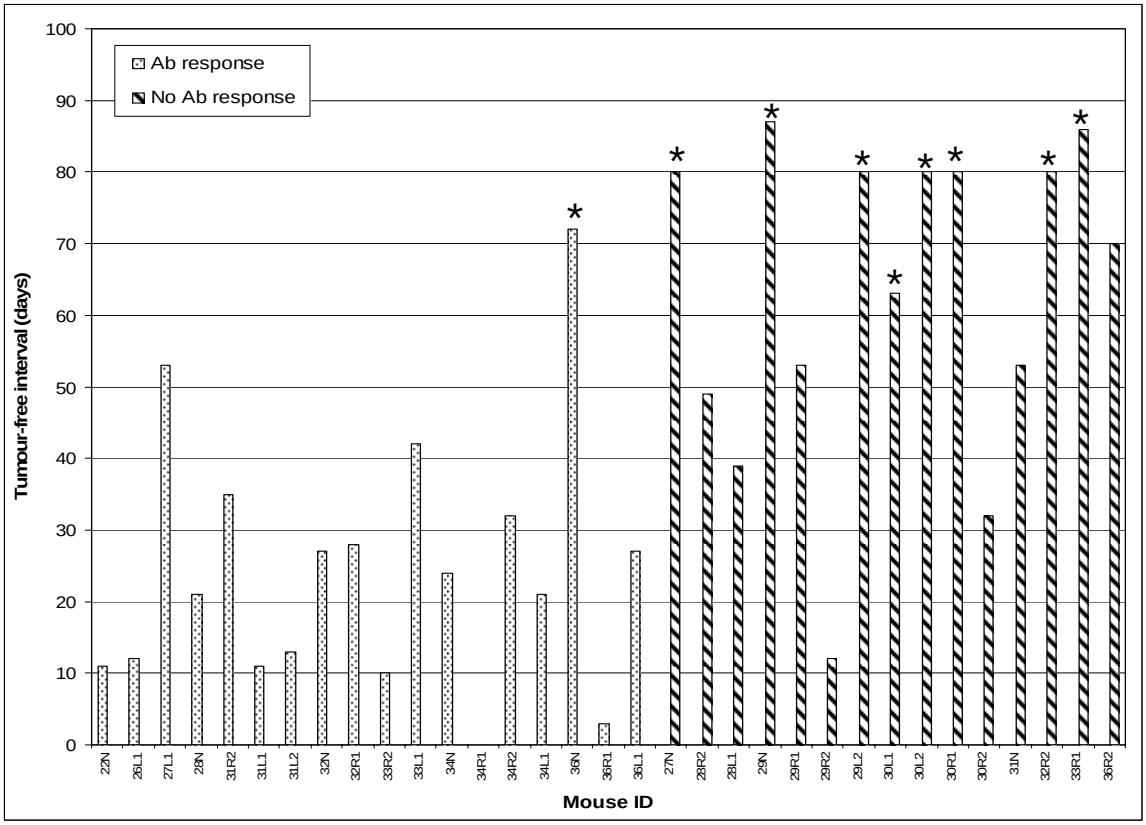

Figure 15. The majority of mice that did not have a PABPN1 antibody (Ab) response had a longer tumour-free interval compared to those mice that did have a PABPN1 antibody response. The * indicates that for these mice, the tumour-free interval was not determined, as the mice were sacrificed on the indicated day for the purpose of immunological analysis.

Another striking difference between mice with and without PABPN1 antibody responses can be observed by examining the tumour growth curves for each group (Figure 16). In general, the majority of the mice with a PABPN1 antibody response had rapidly growing recurrent tumours, as seen from the steep slopes on the graph, while those mice that did not have a PABPN1 antibody response, but did experience tumour recurrence, had tumours that grew more gradually. Thus, contrary to our initial hypothesis, it is evident that PABPN1 antibody responses are associated with poorer outcomes in this model.

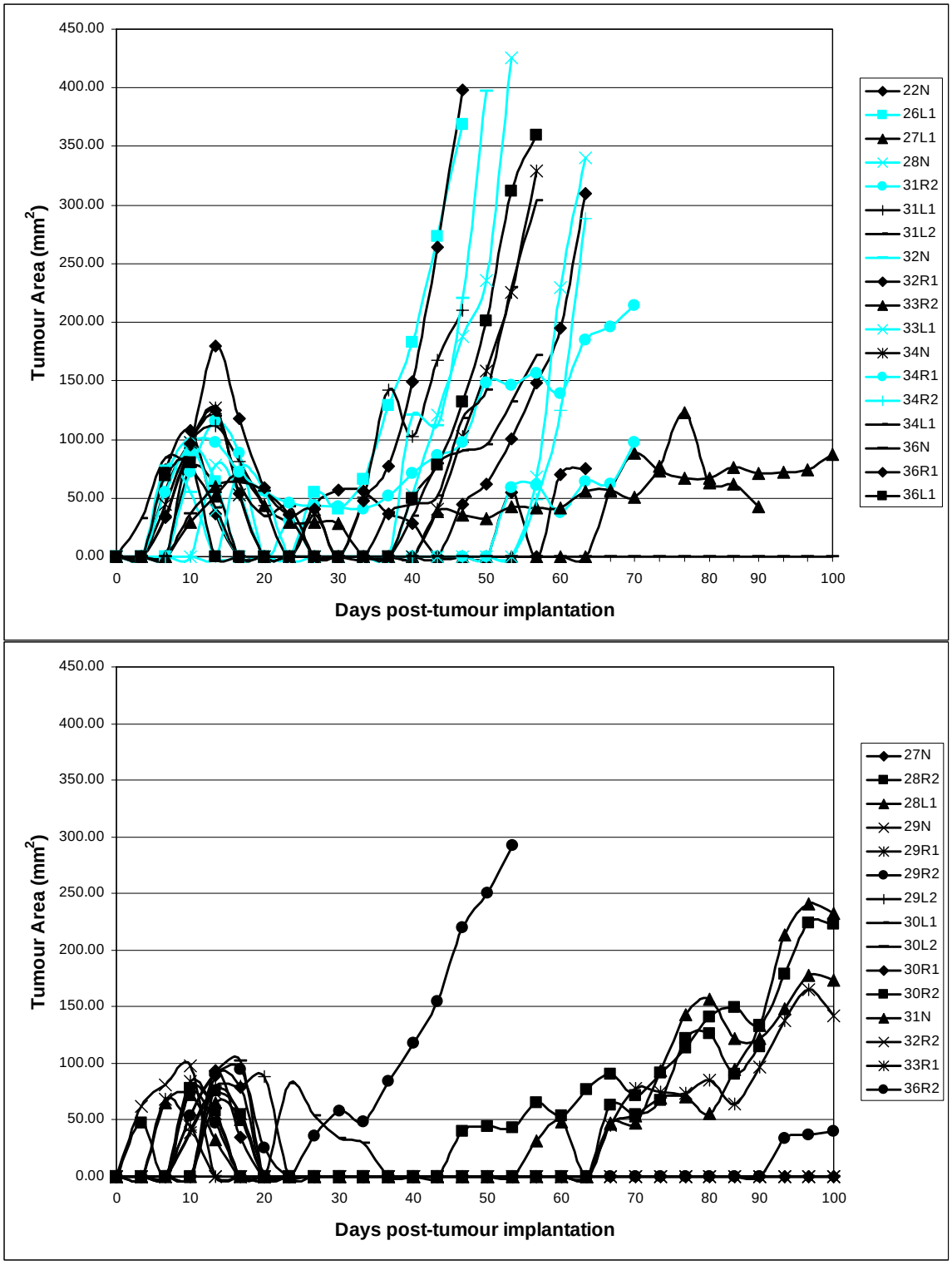

Figure 16. Castrated mice with a PABPN1 antibody response had faster growing recurrent tumours (upper panel) compared to those mice that did not have a PABPN1 antibody response (lower panel). The blue lines on the graph in the upper panel correspond to those mice that had late arising antibody responses following castration (i.e. those occurring > 26 days post-castration).

Immunoblotting against recombinant PABPN1 with sera from each mouse revealed that the average time to develop an antibody response was 26 days post-castration, but individual times ranged from 6-48 days post-castration. Since the range of days in which we first observed the PABPN1 antibody response was broad, we asked whether the time of onset of the PABPN1 antibody response had any relationship to tumour recurrence. We speculated that early antibody responses (i.e. those occurring ≤ 26 days post-castration) might have a protective effect compared to late arising antibody responses (i.e. those occurring > 26 days post-castration). We found that the tumour-free interval for those mice with early antibody responses was similar to the tumour-free interval for those mice with late arising antibody responses, indicating that early antibody responses do not delay the time to tumour recurrence. However, recurrent tumours in mice with early antibody responses appeared to grow more slowly (black lines on upper panel in Figure 16). By contrast, if the antibody response arose later, the recurrent tumours appeared to grow faster (blue lines on upper panel in Figure 16). When we did a formal regression analysis, we found a moderate correlation ($R^2 = 0.5514$) between the day the antibody response occurred and the number of days the mouse carried the recurrent tumour before it had to be sacrificed (Figure 17). Therefore, despite the fact that mice with PABPN1 antibody responses had a shorter mean tumour-free interval than those mice that did not have a PABPN1 antibody response, it appears that this antibody response may have been beneficial in slowing the growth of the recurrent tumour, provided that it occurred shortly after castration.

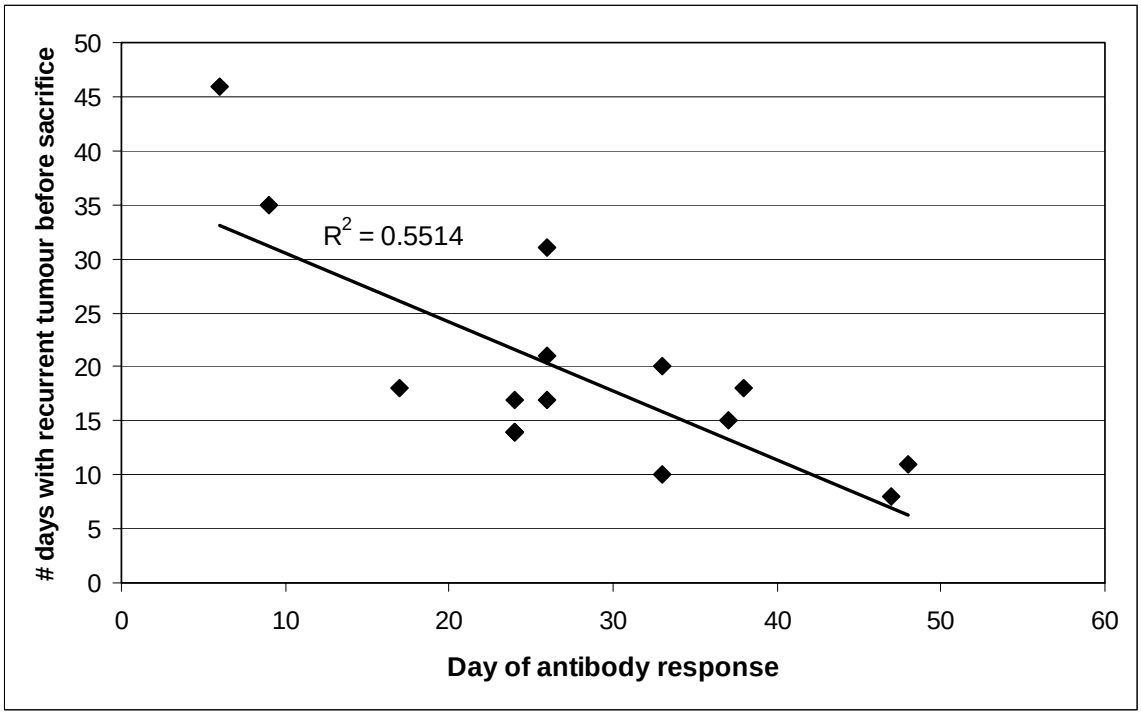

Figure 17. Regression analysis showing a moderate correlation between the day in which the PABPN1 antibody response occurred following castration and the number of days the mouse carried the recurrent tumour before it had to be sacrificed.

We also investigated whether the magnitude of the antibody responses correlated to tumour recurrence. Antibody responses were scored as 0, 1 or 2 based on a subjective assessment of the immunoblot by an independent observer who was blinded to the experimental groups. A regression analysis revealed there to be no correlation between the strength of the PABPN1 antibody response and time to tumour recurrence (R^2 = 0.004), nor was there a correlation between strength of the PABPN1 antibody response and the number of days the mouse carried the recurrent tumour before it had to be sacrificed (R^2 = 0.09).

To determine whether the T cell response against PABPN1 was associated with PABPN1 antibody responses and outcomes, we harvested the spleen from each mouse at the time of sacrifice and used the splenocytes in an IFN-γ ELISPOT assay to measure the magnitude of the PABPN1-specific T cell response. Mice with PABPN1 antibody responses had stronger T cell responses (mean of 406 IFN-γ spot-forming cells per million cells), compared to mice that did not have a PABPN1 antibody response (mean of 38 IFN-γ spot-forming cells per million cells) (Figure 18). Accordingly, mice with recurrent tumours had exceedingly stronger PABPN1-specific T cell responses (mean of 335 IFN-γ spot-forming cells per million cells), compared to mice that did not have recurrent tumours (mean of 36 IFN-γ spot-forming cells per million cells) (Figure 19). Thus, contrary to my initial hypothesis, both antibody and T cell responses against PABPN1 were correlated with poorer outcomes.

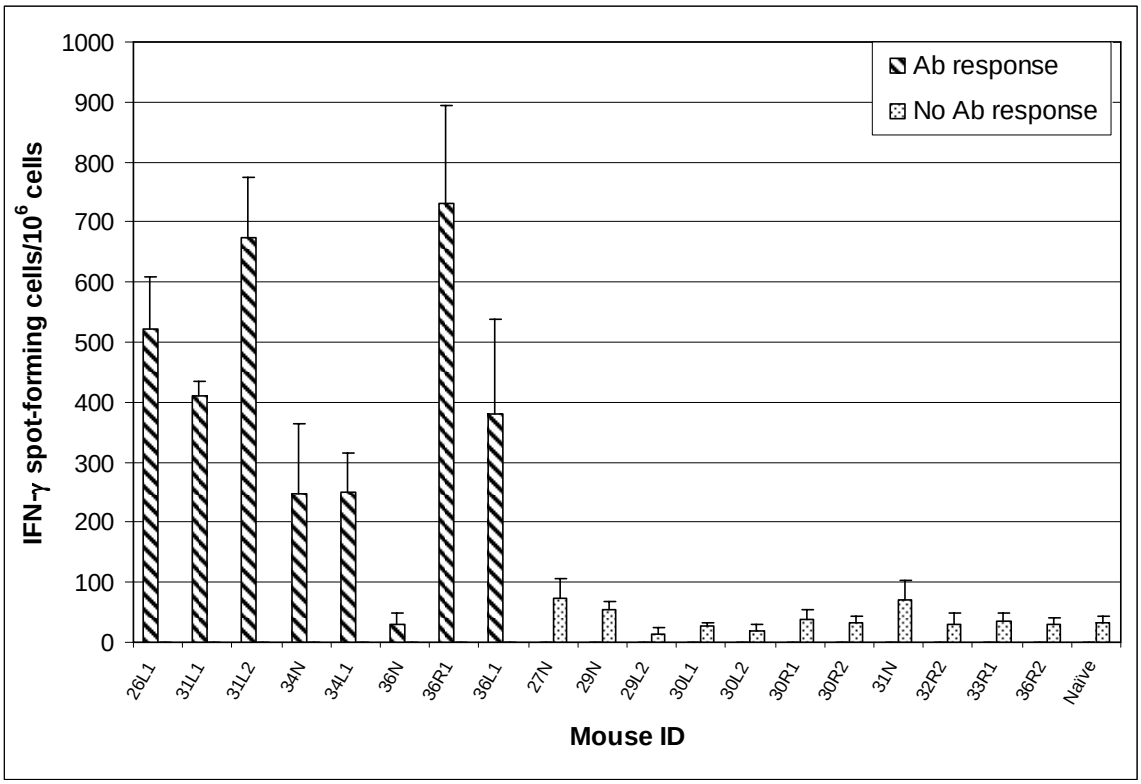

Figure 18. Castrated mice that had a PABPN1 antibody (Ab) response generally had a larger PABPN1-specific T cell response compared to those mice that did not have a PABPN1 antibody response. For each mouse shown on the graph, fresh splenocytes were used in the ELISPOT assay, which was run in triplicate, with the values being averaged and the standard deviation calculated.

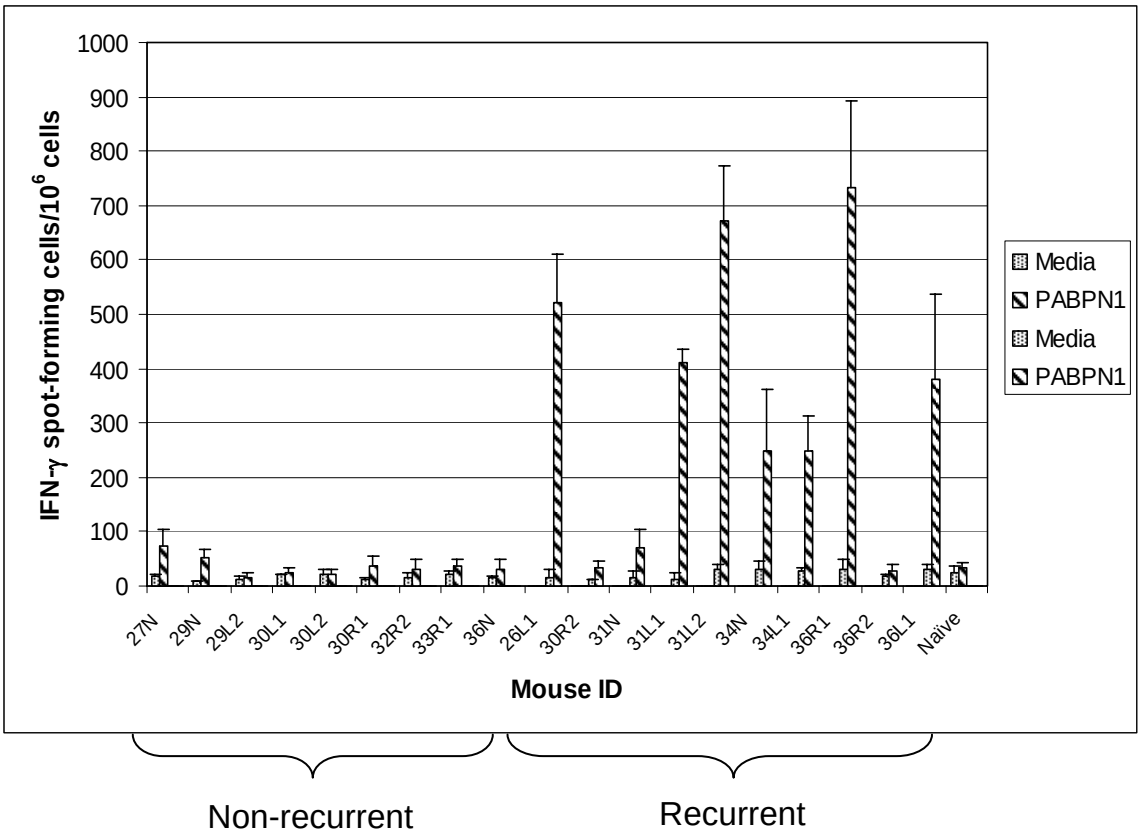

Figure 19. Castrated mice with recurrent tumours generally had a larger PABPN1-specific T cell response compared to those mice that remained tumour-free for the duration of the experiment. For each mouse shown on the graph, fresh splenocytes were used in the ELISPOT assay, which was run in triplicate, with the values being averaged and the standard deviation calculated. The splenocytes were stimulated with media as a negative control.

An interesting observation that I made while harvesting the spleens was that mice with recurrent tumours had splenomegaly compared to mice that did not have recurrent tumours. This observation was verified by the mean splenocyte counts for the recurrent mice (1.99×10^8 splenocytes per spleen) versus the non-recurrent mice (1.56×10^8 splenocytes per spleen). I interpreted this finding to mean that proliferation of PABPN1-specific T cells *in vivo* lead to splenomegaly, which was confirmed by the results from the IFN-γ ELISPOT assays, which showed that mice with recurrent tumours had stronger PABPN1-specific T cell responses.

Possible immune escape mechanisms used by Shionogi tumours

The unexpected finding that PABPN1-specific antibody and T cell responses were associated with unfavourable outcomes raised the issue of whether recurrent Shionogi tumours still express the target antigen PABPN1. Therefore, we used immunoblotting to analyze the expression of PABPN1 in 15 different recurrent tumours compared to a primary tumour. Although the expression of PABPN1 did vary slightly between some of the recurrent tumours compared to the primary tumour, all of the recurrent tumours that we analyzed were positive for expression (Figure 20). Therefore, loss of PABPN1 expression does not seem to be a likely escape mechanism.

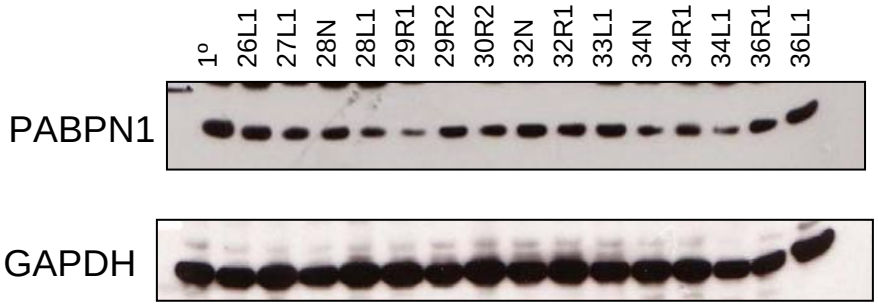

Figure 20. PABPN1 expression does not vary significantly in primary versus recurrent Shionogi tumours. 20 µg of each tumour lysate was loaded per lane. The blot was screened with serum from a PABPN1-immunized mouse. GAPDH served as the loading control.

Since mice with recurrent tumours had a substantial PABPN1-specific T cell response, and the tumours still expressed antigen, we questioned whether these T cells trafficked to the tumour. Anti-CD3 staining of the recurrent tumours by IHC revealed a plethora of CD3+ T cells at the periphery of the tumour and in the surrounding stroma, however, very few CD3+ T cells infiltrated the epithelial component of the tumour (Figure 21). This observation may explain why the PABPN1-specific T cells were not effective at eradicating recurrent tumours.

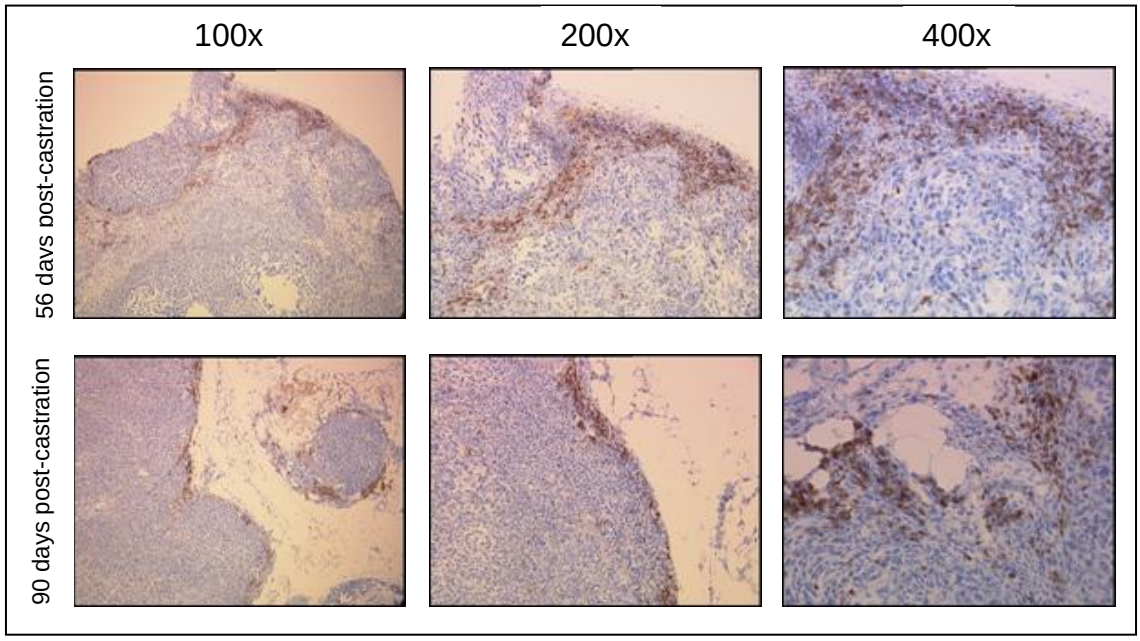

Figure 21. Representative recurrent tumours stained with anti-CD3 from one mouse sacrificed on day 56 post-castration and one mouse sacrificed on day 90 post-castration show that the CD3+ T cells are mainly confined to the periphery of the tumours and surrounding stroma.

Discussion

We recently showed that standard treatments induce tumour-specific antibody responses in a significant proportion of human prostate cancer patients (26). However, it is not yet known whether these treatment-associated immune responses lead to improved clinical outcomes. To address this question, we utilized the murine Shionogi carcinoma model since we observed a treatment-induced antibody response in a large proportion of mice in a preliminary experiment using this model. We hypothesized that castrated mice that mount treatment-associated tumour-specific immune responses will have delayed time to tumour recurrence and prolonged survival, relative to those mice that do not mount treatment-associated tumour-specific immune responses. First, we identified and cloned an antigen, PABPN1, that a significant proportion of castrated mice mounted an antibody response against, in order to determine if castration also induced a T cell response. Typically, we found that castrated mice that had a PABPN1-specific antibody response also mounted a PABPN1-specific T cell response. Unexpectedly, we found that castrated mice with PABPN1-specific antibody and T cell responses had poorer outcomes relative to those castrated mice that did not mount an immune response against PABPN1. Overall, these mice had a shorter mean tumour-free interval and were more likely to experience tumour recurrence relative to those mice that did not mount an immune response against PABPN1. The primary immune response that was generated following castration seemed to be beneficial because we observed dense infiltration of CD3+ intratumoural cells between 7-14 days post-castration, which coincided with tumour regression. However, when the tumours recurred, it was evident that the PABPN1-

specific antibody and T cell response did not slow the growth rate of the recurrent tumour, unless the antibody response arose shortly after castration. One possible explanation for why PABPN1-specific T cell responses were not effective at eradicating recurrent tumours is because we observed by IHC that the CD3+ T cells were mainly found in the periphery of the recurrent tumours and surrounding stroma. Nonetheless, this observation does not explain why the majority of castrated mice that did not mount PABPN1-specific antibody and T cell responses had better outcomes.

We found it intriguing that castrated mice with PABPN1-specific antibody responses had a shorter mean tumour-free interval compared to those castrated mice that did not have a PABPN1 antibody response. Likewise, we found it interesting that the majority of mice with recurrent tumours had an antibody response against PABPN1, whereas only a single mouse that remained tumour-free for the duration of the experiment had a PABPN1-specific antibody response. We speculated that the PABPN1 antibody response may be a marker for tumour recurrence, since we observed the PABPN1 antibody response in 63% (10/16) of castrated mice before the recurrent tumour was detected. A regression analysis showed that if the PABPN1 antibody response occurred well before tumour recurrence, it was capable of slowing the growth rate of the recurrent tumour and prolonging survival. However, if the PABPN1-specific antibody response occurred a few weeks after castration and shortly before tumour recurrence, we speculate that was likely not strong enough to slow the growth of the recurrent tumour.

Examination of the PABPN1-specific T cell response by IFN-γ ELISPOT assays showed that the majority of the mice with a PABPN1 antibody response had a significantly stronger PABPN1-specific T cell response compared to those mice that did

not have a PABPN1 antibody response. Accordingly, the majority of the mice that experienced tumour recurrence had exceedingly stronger PABPN1-specific T cell responses compared to those mice that remained tumour-free until the end of the experiment. One possible explanation for this finding is that the recurrent tumour triggered a memory T cell response. Unfortunately, this theory could not be confirmed by our IFN-γ ELISPOT data since the assay does not discriminate between primary and memory responses (9). The memory T cell response may not have been effective at eradicating the recurrent tumour due to the fact that the majority of the T cells could not infiltrate the tumour, as shown by anti-CD3 staining. Additionally, we speculate that the memory T cell response is made up of predominantly CD4+ T helper cells since we used whole antigen to stimulate the T cells in the IFN-γ ELISPOT assays. Although there can be cross-presentation of extracellular antigenic peptides to CD8+ T cells, typically whole antigen is taken up and processed by dendritic cells and peptides are presented in the context of MHC class II molecules, which are recognized by CD4+ T helper cells (9, 36). Essentially, the consequence of having a response that mainly consists of CD4+ T helper cells is that they are not as effective at killing tumour cells compared to cytotoxic CD8+ T cells. In fact, McArdle *et al.* (23) showed that the presence of increased CD4+ T-lymphocyte infiltration was associated with poor outcome, independent of stage, in patients with prostate cancer. We are currently doing IFN-γ ELISPOT assays with CD4+ versus CD8+ T cells to test our idea that the memory T cell response is primarily made up of CD4+ T helper cells.

We were intrigued by the fact that in the murine Shionogi carcinoma model, castration induced such a strong immune response against PABPN1, which is an

abundant, ubiquitously expressed self-antigen (46, GeneNote Version 2.1). This is not the first time this phenomenon has been observed. Recently, Savage *et al.* (52) identified a naturally arising CD8+ T cell response that was reactive to a peptide derived from histone H4, an ubiquitously expressed protein, in the male transgenic adenocarcinoma of mouse prostate model. Interestingly, they found that these antigen-specific T cells were able to normally traffic to the tumour, exhibited increased expression of the T cell activation marker CD44, but did not express the cytotoxic effector molecule granzyme B. Possible explanations for why the immune system is mounting a response against self-antigens, when normally it is tolerant to them, may be related to the pattern of antigen expression or changes occurring in the tumour microenvironment following treatment (52). Nonetheless, the monitoring of PABPN1-specific immune responses in the murine Shionogi carcinoma model will serve as a valuable tool for further understanding the relationship between treatment-induced anti-tumour immune responses and outcomes.

We have identified some unresolved issues with our study. First of all, it would have been useful to know what proportion, if any, of the intratumoural CD3+ T cells that we observed in the tumours between days 7-14 post-castration were PABPN1-specific. If the intratumoural CD3+ T cells were specific for PABPN1, it would provide a better indication of their functionality. We are presuming that the intratumoural CD3+ T cells are functional since the tumours regressed during this time period, however, there is a possibility that they are bystanders and were somehow recruited to the tumour site by factors present in the tumour microenvironment. Furthermore, determining that the intratumoural CD3+ T cells are PABPN1-specific would demonstrate the usefulness of this antigen as a target of the immune response. We would also like to identify what

mechanism the intratumoural CD3+ T cells are using to kill Shionogi tumour cells, if in fact they are contributing to tumour regression. By IHC staining for granzyme B, we determined that the intratumoural CD3+ T cells observed on days 7-14 post-castration lacked this cytolytic effector molecule, however, there are other methods by which T cells kill their targets, including Fas-mediated cell death (48). Another possibility is that the Tregs we observed in the Shionogi tumours between 7-14 days post-castration may have down-regulated the functions of the effector T cells (53). Secondly, we would have also liked to confirm our hypothesis that the memory T cell response is predominantly made up of CD4+ T helper cells. Although we did find that more CD8+ T cells were present within the tumours around day 7 post-castration, the balance may have shifted in the memory T cell response, such that it primarily became more of a CD4+ T helper response. We have also considered the possibility that the memory T cell response may be dominated by tolerant or malfunctioning T cells that have a suppressive phenotype or senescent features (54). This would provide a possible explanation for why castrated mice that did not have a T cell response had better outcomes. Finally, we would have liked to gain a better understanding as to why the majority of the CD3+ T cells were restricted to the periphery of the recurrent tumours. We ruled out the possibility of PABPN1 down-regulation by the recurrent tumours, however, there are several more tumour immune evasion mechanisms that we would like to investigate. Some of these include decreased expression of MHC class I molecules, which would impair T cell recognition of tumour antigens, and the secretion of immunosuppressive cytokines, such as IL-10 and transforming growth factor-β, into the tumour microenvironment by the tumour cells or Tregs (6, 8, 53, 55). By understanding some of the possible Shionogi

tumour immune evasion mechanisms, we can administer T cell activating cytokines, such as IL-15, in future experiments to overcome these hurdles (56, 57). Overall, recognizing the limitations with our study has allowed us to improve upon planning future experiments.

Despite the fact that antibody and T cell responses against PABPN1 were associated with poorer outcomes in the murine Shionogi carcinoma model, we have numerous experiments planned for the future using this model to further understand the association between treatment-induced immune responses and outcomes. First of all, we are currently working on an experiment which involves injecting DD/S mice with anti-CD4 and/or anti-CD8 antibodies to deplete the CD4+ and/or CD8+ T cells and determine how this influences outcome following castration. Not only will this depletion experiment allow us to further define the functionality of T cells with respect to their contribution to tumour regression and tumour recurrence, but it will also allow us to determine the proportions of CD4+ and CD8+ T cells that make up the T cell response. If we find that the T cell response is mainly a CD4+ T helper response, which we speculate, then we can utilize various methods to sway the response towards a cytotoxic CD8+ T cell response. One method that we have already tested and know is capable of producing a moderate PABPN1-specific T cell response, is to vaccinate DD/S mice with PABPN1 + poly I:C. Polyinosinic:polycytidylic acid is an analog of viral dsRNA and a toll-like receptor ligand that has been shown to increase the number and function of antigen-specific CD8+ T cells after concomitant administration with a peptide vaccine in a mouse model (58). Having a predominantly CD8+ T cell response present at the time of tumour inoculation might augment the castration-induced immune response, such that

tumour recurrence is delayed or absent. Finally, we would like to gain insight as to why not having a treatment-induced tumour-specific immune response leads to a better outcome. We considered the possibility that the T cell response switches from a T helper1 (T_{H1}) response to a T helper2 (T_{H2}) response. T_{H1} cells, characterized by the secretion of IFN-γ and tumour necrosis factor-α, are primarily responsible for activating and regulating the development and persistence of cytotoxic T cells. Thus, T_{H1} anti-tumour responses are typically associated with favourable outcomes. Conversely, T_{H2} cells, characterized by the secretion of IL-4 and IL-10, favour a predominantly humoral response, and down-regulate anti-tumour immunity through IL-10-mediated inhibition of dendritic cell antigen processing and presentation and activation of Tregs (47, 59). We speculated that mice with a predominantly T_{H2} response, and hence those mice that had a PABPN1-specific antibody response, had poorer outcomes relative to those mice that had a predominantly T_{H1} response, and hence those mice that did not have a PABPN1-specific antibody response. However, since our ELISPOT assay measured the release of IFN-γ, a cytokine secreted by T_{H1} cells, and the vast majority of mice with a PABPN1-specific antibody response had a strong PABPN1-specific T cell response, we ruled out the possibility of this switch (47).

To our knowledge, this is the first study that showed that treatment-induced, antigen-specific T cell responses are associated with unfavourable outcomes. In the chronic setting of certain diseases, T cell responses contribute to the pathogenesis of cancer. For example, in hepatitis B and C, multiple types of cytotoxic lymphocytes promote hepatocyte damage and fibrosis through direct cellular toxicity and the release of inflammatory cytokines (60). Likewise, the T cell response directed against chronic

Helicobacter pylori infection is believed to contribute to the development of gastric adenocarcinoma (61). In our study, we are not sure whether the PABPN1-specfic T cell response contributed to tumour recurrence or if it was attempting to eradicate the recurrent tumour but was not successful due to immune escape mechanisms employed by the tumour, such as the secretion of immunosuppressive cytokines. Regardless of the reason, the absence of a PABPN1-specific T cell response was associated with a more favourable outcome in the murine Shionogi carcinoma model.

To our knowledge, this is the first study that showed that treatment-induced antigen-specific antibody responses are associated with unfavourable outcomes. Although it has been shown that antibody responses against p53 are associated with a poor prognosis in several types of cancer, including non-small cell lung, ovarian, bladder, and oesophageal, these p53-specific antibody responses were either present before treatment or not shown to be treatment-induced (62-66). In contrast, for a number of different cancers, including melanoma, gastric, glioblastoma, and breast it has been reported that patients who mounted antibody responses against particular self-antigens appeared to have an improved prognosis (67-71). This conflicts with our finding that PABPN1-specific antibody responses are associated with unfavourable outcomes in the murine Shionogi carcinoma model.

Considering that immune responses are protective and beneficial, except in the case of autoimmunity, we hypothesized that treatment-induced anti-tumour antibody and T cell responses would lead to better outcomes (8). However, our experiments using the murine Shionogi carcinoma model provided strong evidence that in fact they appear to be associated with poorer outcomes. Although further investigation is needed to understand

the relationship between treatment-induced anti-tumour immune responses and outcomes, if the findings from our experiments hold true for human cancer patients, then perhaps we need to think about ways to dampen treatment-induced immune responses rather than augment them.

Bibliography

1. Hoeppner, L. H., J. A. Dubovsky, E. J. Dunphy, and D. G. McNeel. 2006. Humoral immune responses to testis antigens in sera from patients with prostate cancer. *Cancer Immun* 6:1.

2. Garcia-Hernandez Mde, L., A. Gray, B. Hubby, and W. M. Kast. 2007. In vivo effects of vaccination with six-transmembrane epithelial antigen of the prostate: a candidate antigen for treating prostate cancer. *Cancer Res* 67:1344-1351.

3. Ludgate, C. M., D. C. Bishop, H. Pai, B. Eldridge, J. Lim, E. Berthelet, P. Blood, G. B. Piercy, and G. Steinhoff. 2005. Neoadjuvant hormone therapy and external-beam radiation for localized high-risk prostate cancer: the importance of PSA nadir before radiation. *Int J Radiat Oncol Biol Phys* 62:1309-1315.

4. Attard, G., D. Sarker, A. Reid, R. Molife, C. Parker, and J. S. de Bono. 2006. Improving the outcome of patients with castration-resistant prostate cancer through rational drug development. *Br J Cancer* 95:767-774.

5. Di Lorenzo, G., R. Autorino, W. D. Figg, and S. De Placido. 2007. Hormone-refractory prostate cancer: where are we going? *Drugs* 67:1109-1124.

6. Vieweg, J. 2007. Immunotherapy for advanced prostate cancer. *Rev Urol* 9 Suppl 1:S29-38.

7. Small, E. J., N. Sacks, J. Nemunaitis, W. J. Urba, E. Dula, A. S. Centeno, W. G. Nelson, D. Ando, C. Howard, F. Borellini, M. Nguyen, K. Hege, and J. W. Simons. 2007. Granulocyte macrophage colony-stimulating factor--secreting allogeneic cellular immunotherapy for hormone-refractory prostate cancer. *Clin Cancer Res* 13:3883-3891.

8. Zitvogel, L., A. Tesniere, and G. Kroemer. 2006. Cancer despite immunosurveillance: immunoselection and immunosubversion. *Nat Rev Immunol* 6:715-727.

9. Whiteside, T. L. 2000. Monitoring of antigen-specific cytolytic T lymphocytes in cancer patients receiving immunotherapy. *Clin Diagn Lab Immunol* 7:327-332.

10. Simons, J. W., and N. Sacks. 2006. Granulocyte-macrophage colony-stimulating factor-transduced allogeneic cancer cellular immunotherapy: the GVAX vaccine for prostate cancer. *Urol Oncol* 24:419-424.

11. Mukhopadhaya, A., J. Mendecki, X. Dong, L. Liu, S. Kalnicki, M. Garg, A. Alfieri, and C. Guha. 2007. Localized hyperthermia combined with intratumoral dendritic cells induces systemic antitumor immunity. *Cancer Res* 67:7798-7806.

12. Small, E. J., P. F. Schellhammer, C. S. Higano, C. H. Redfern, J. J. Nemunaitis, F. H. Valone, S. S. Verjee, L. A. Jones, and R. M. Hershberg. 2006. Placebo-controlled phase III trial of immunologic therapy with sipuleucel-T (APC8015) in patients with metastatic, asymptomatic hormone refractory prostate cancer. *J Clin Oncol* 24:3089-3094.

13. Mercader, M., B. K. Bodner, M. T. Moser, P. S. Kwon, E. S. Park, R. G. Manecke, T. M. Ellis, E. M. Wojcik, D. Yang, R. C. Flanigan, W. B. Waters, W. M. Kast, and E. D. Kwon. 2001. T cell infiltration of the prostate induced by androgen withdrawal in patients with prostate cancer. *Proc Natl Acad Sci U S A* 98:14565-14570.

14. McBride, W. H., C. S. Chiang, J. L. Olson, C. C. Wang, J. H. Hong, F. Pajonk, G. J. Dougherty, K. S. Iwamoto, M. Pervan, and Y. P. Liao. 2004. A sense of danger from radiation. *Radiat Res* 162:1-19.

15. Friedman, E. J. 2002. Immune modulation by ionizing radiation and its implications for cancer immunotherapy. *Curr Pharm Des* 8:1765-1780.

16. Demaria, S., N. Bhardwaj, W. H. McBride, and S. C. Formenti. 2005. Combining radiotherapy and immunotherapy: a revived partnership. *Int J Radiat Oncol Biol Phys* 63:655-666.

17. Garnett, C. T., C. Palena, M. Chakraborty, K. Y. Tsang, J. Schlom, and J. W. Hodge. 2004. Sublethal irradiation of human tumor cells modulates phenotype resulting in enhanced killing by cytotoxic T lymphocytes. *Cancer Res* 64:7985-7994.

18. Chakraborty, M., S. I. Abrams, K. Camphausen, K. Liu, T. Scott, C. N. Coleman, and J. W. Hodge. 2003. Irradiation of tumor cells up-regulates Fas and enhances CTL lytic activity and CTL adoptive immunotherapy. *J Immunol* 170:6338-6347.

19. McNeel, D. G., L. D. Nguyen, B. E. Storer, R. Vessella, P. H. Lange, and M. L. Disis. 2000. Antibody immunity to prostate cancer associated antigens can be detected in the serum of patients with prostate cancer. *J Urol* 164:1825-1829.

20. Wang, X., J. Yu, A. Sreekumar, S. Varambally, R. Shen, D. Giacherio, R. Mehra, J. E. Montie, K. J. Pienta, M. G. Sanda, P. W. Kantoff, M. A. Rubin, J. T. Wei, D. Ghosh, and A. M. Chinnaiyan. 2005. Autoantibody signatures in prostate cancer. *N Engl J Med* 353:1224-1235.

21. Anderson, M. J., K. Shafer-Weaver, N. M. Greenberg, and A. A. Hurwitz. 2007. Tolerization of tumor-specific T cells despite efficient initial priming in a primary murine model of prostate cancer. *J Immunol* 178:1268-1276.

22. Zhang, L., J. R. Conejo-Garcia, D. Katsaros, P. A. Gimotty, M. Massobrio, G. Regnani, A. Makrigiannakis, H. Gray, K. Schlienger, M. N. Liebman, S. C. Rubin, and G. Coukos. 2003. Intratumoral T cells, recurrence, and survival in epithelial ovarian cancer. *N Engl J Med* 348:203-213.

23. McArdle, P. A., K. Canna, D. C. McMillan, A. M. McNicol, R. Campbell, and M. A. Underwood. 2004. The relationship between T-lymphocyte subset infiltration and survival in patients with prostate cancer. *Br J Cancer* 91:541-543.

24. Galon, J., A. Costes, F. Sanchez-Cabo, A. Kirilovsky, B. Mlecnik, C. Lagorce-Pages, M. Tosolini, M. Camus, A. Berger, P. Wind, F. Zinzindohoue, P. Bruneval, P. H. Cugnenc, Z. Trajanoski, W. H. Fridman, and F. Pages. 2006. Type, density, and location of immune cells within human colorectal tumors predict clinical outcome. *Science* 313:1960-1964.

25. Liakou, C. I., S. Narayanan, D. Ng Tang, C. J. Logothetis, and P. Sharma. 2007. Focus on TILs: Prognostic significance of tumor infiltrating lymphocytes in human bladder cancer. *Cancer Immun* 7:10.

26. Nesslinger, N. J., R. A. Sahota, B. Stone, K. Johnson, N. Chima, C. King, D. Rasmussen, D. Bishop, P. S. Rennie, M. Gleave, P. Blood, H. Pai, C. Ludgate, and B. H. Nelson. 2007. Standard treatments induce antigen-specific immune responses in prostate cancer. *Clin Cancer Res* 13:1493-1502.

27. Sahin, U., O. Tureci, H. Schmitt, B. Cochlovius, T. Johannes, R. Schmits, F. Stenner, G. Luo, I. Schobert, and M. Pfreundschuh. 1995. Human neoplasms elicit multiple specific immune responses in the autologous host. *Proc Natl Acad Sci U S A* 92:11810-11813.

28. Fernandez Madrid, F., N. Tang, H. Alansari, R. L. Karvonen, and J. E. Tomkiel. 2005. Improved approach to identify cancer-associated autoantigens. *Autoimmun Rev* 4:230-235.

29. Miles, A. K., A. Rogers, G. Li, R. Seth, D. Powe, S. E. McArdle, T. A. McCulloch, M. C. Bishop, and R. C. Rees. 2007. Identification of a novel prostate cancer-associated tumor antigen. *Prostate* 67:274-287.

30. Alsoe, L., J. E. Stacy, A. Fossa, S. Funderud, O. H. Brekke, and G. Gaudernack. 2008. Identification of prostate cancer antigens by automated high-throughput filter immunoscreening. *J Immunol Methods* 330:12-23.

31. Minesita, T., and K. Yamaguchi. 1965. An androgen-dependent mouse mammary tumor. *Cancer Res* 25:1168-1175.

32. Skov, K., H. Adomat, M. Bowden, W. Dragowska, M. Gleave, C. J. Koch, J. Woo, and D. T. Yapp. 2004. Hypoxia in the androgen-dependent Shionogi model for prostate cancer at three stages. *Radiat Res* 162:547-553.

33. So, A. I., M. Bowden, and M. Gleave. 2004. Effect of time of castration and tumour volume on time to androgen-independent recurrence in Shionogi tumours. *BJU Int* 93:845-850.

34. Bruchovsky, N., P. S. Rennie, A. J. Coldman, S. L. Goldenberg, M. To, and D. Lawson. 1990. Effects of androgen withdrawal on the stem cell composition of the Shionogi carcinoma. *Cancer Res* 50:2275-2282.

35. Yoshikawa, T., Y. Kitamura, N. Uchida, K. Yamaguchi, and K. Matsumoto. 1983. Effect of adjuvant endocrine and adjuvant chemoendocrine therapies on metastasis of androgen-dependent Shionogi carcinoma 115. *Cancer Res* 43:4525-4529.

36. Gajewski, T. F. 2000. Monitoring specific T-cell responses to melanoma vaccines: ELISPOT, tetramers, and beyond. *Clin Diagn Lab Immunol* 7:141-144.

37. Rosenberg, Y. J. 1982. Isotype-specific T cell regulation of immunoglobulin expression. *Immunol Rev* 67:33-58.

38. van der Bruggen, P., C. Traversari, P. Chomez, C. Lurquin, E. De Plaen, B. Van den Eynde, A. Knuth, and T. Boon. 1991. A gene encoding an antigen recognized by cytolytic T lymphocytes on a human melanoma. *Science* 254:1643-1647.

39. Jager, E., Y. T. Chen, J. W. Drijfhout, J. Karbach, M. Ringhoffer, D. Jager, M. Arand, H. Wada, Y. Noguchi, E. Stockert, L. J. Old, and A. Knuth. 1998. Simultaneous humoral and cellular immune response against cancer-testis antigen NY-ESO-1: definition of human histocompatibility leukocyte antigen (HLA)-A2-binding peptide epitopes. *J Exp Med* 187:265-270.

40. Hoffmann, T. K., A. D. Donnenberg, S. D. Finkelstein, V. S. Donnenberg, U. Friebe-Hoffmann, E. N. Myers, E. Appella, A. B. DeLeo, and T. L. Whiteside. 2002. Frequencies of tetramer+ T cells specific for the wild-type sequence p53(264-272) peptide in the circulation of patients with head and neck cancer. *Cancer Res* 62:3521-3529.

41. Takahashi, Y., M. Karbowski, H. Yamaguchi, A. Kazi, J. Wu, S. M. Sebti, R. J. Youle, and H. G. Wang. 2005. Loss of Bif-1 suppresses Bax/Bak conformational change and mitochondrial apoptosis. *Mol Cell Biol* 25:9369-9382.

42. Goward, C. R., and D. J. Nicholls. 1994. Malate dehydrogenase: a model for structure, evolution, and catalysis. *Protein Sci* 3:1883-1888.

43. Chung, S., Z. Zhou, K. A. Huddleston, D. A. Harrison, R. Reed, T. A. Coleman, and B. C. Rymond. 2002. Crooked neck is a component of the human spliceosome and implicated in the splicing process. *Biochim Biophys Acta* 1576:287-297.

44. Hosoda, N., F. Lejeune, and L. E. Maquat. 2006. Evidence that poly(A) binding protein C1 binds nuclear pre-mRNA poly(A) tails. *Mol Cell Biol* 26:3085-3097.

45. Nemeth, A., S. Krause, D. Blank, A. Jenny, P. Jeno, A. Lustig, and E. Wahle. 1995. Isolation of genomic and cDNA clones encoding bovine poly(A) binding protein II. *Nucleic Acids Res* 23:4034-4041.

46. Shmueli, O., S. Horn-Saban, V. Chalifa-Caspi, M. Shmoish, R. Ophir, H. Benjamin-Rodrig, M. Safran, E. Domany, and D. Lancet. 2003. GeneNote: whole genome expression profiles in normal human tissues. *C R Biol* 326:1067-1072.

47. Knutson, K. L., and M. L. Disis. 2005. Tumor antigen-specific T helper cells in cancer immunity and immunotherapy. *Cancer Immunol Immunother* 54:721-728.

48. Lieberman, J. 2003. The ABCs of granule-mediated cytotoxicity: new weapons in the arsenal. *Nat Rev Immunol* 3:361-370.

49. Curiel, T. J., G. Coukos, L. Zou, X. Alvarez, P. Cheng, P. Mottram, M. Evdemon-Hogan, J. R. Conejo-Garcia, L. Zhang, M. Burow, Y. Zhu, S. Wei, I. Kryczek, B. Daniel, A. Gordon, L. Myers, A. Lackner, M. L. Disis, K. L. Knutson, L. Chen, and W. Zou. 2004. Specific recruitment of regulatory T cells in ovarian carcinoma fosters immune privilege and predicts reduced survival. *Nat Med* 10:942-949.

50. Torlakovic, E., A. Slipicevic, C. Robinson, J. F. DeCoteau, G. C. Alfsen, M. Vyberg, R. Chibbar, and V. A. Florenes. 2006. Pax-5 expression in nonhematopoietic tissues. *Am J Clin Pathol* 126:798-804.

51. Roden, A. C., M. T. Moser, S. D. Tri, M. Mercader, S. M. Kuntz, H. Dong, A. A. Hurwitz, D. J. McKean, E. Celis, B. C. Leibovich, J. P. Allison, and E. D. Kwon. 2004. Augmentation of T cell levels and responses induced by androgen deprivation. *J Immunol* 173:6098-6108.

52. Savage, P. A., K. Vosseller, C. Kang, K. Larimore, E. Riedel, K. Wojnoonski, A. A. Jungbluth, and J. P. Allison. 2008. Recognition of a ubiquitous self antigen by prostate cancer-infiltrating CD8+ T lymphocytes. *Science* 319:215-220.

53. Miller, A. M., K. Lundberg, V. Ozenci, A. H. Banham, M. Hellstrom, L. Egevad, and P. Pisa. 2006. CD4+CD25high T cells are enriched in the tumor and peripheral blood of prostate cancer patients. *J Immunol* 177:7398-7405.

54. Montes, C. L., A. I. Chapoval, J. Nelson, V. Orhue, X. Zhang, D. H. Schulze, S. E. Strome, and B. R. Gastman. 2008. Tumor-induced senescent T cells with suppressor function: a potential form of tumor immune evasion. *Cancer Res* 68:870-879.

55. Miller, A. M., and P. Pisa. 2007. Tumor escape mechanisms in prostate cancer. *Cancer Immunol Immunother* 56:81-87.

56. Stoklasek, T. A., K. S. Schluns, and L. Lefrancois. 2006. Combined IL-15/IL-15Ralpha immunotherapy maximizes IL-15 activity in vivo. *J Immunol* 177:6072-6080.

57. Rubinstein, M. P., A. N. Kadima, M. L. Salem, C. L. Nguyen, W. E. Gillanders, and D. J. Cole. 2002. Systemic administration of IL-15 augments the antigen-specific primary CD8+ T cell response following vaccination with peptide-pulsed dendritic cells. *J Immunol* 169:4928-4935.

58. Salem, M. L., A. N. Kadima, D. J. Cole, and W. E. Gillanders. 2005. Defining the antigen-specific T-cell response to vaccination and poly(I:C)/TLR3 signaling: evidence of enhanced primary and memory CD8 T-cell responses and antitumor immunity. *J Immunother (1997)* 28:220-228.

59. Ellyard, J. I., L. Simson, and C. R. Parish. 2007. Th2-mediated anti-tumour immunity: friend or foe? *Tissue Antigens* 70:1-11.

60. Mengshol, J. A., L. Golden-Mason, and H. R. Rosen. 2007. Mechanisms of Disease: HCV-induced liver injury. *Nat Clin Pract Gastroenterol Hepatol* 4:622-634.

61. Lundin, B. S., K. Enarsson, B. Kindlund, A. Lundgren, E. Johnsson, M. Quiding-Jarbrink, and A. M. Svennerholm. 2007. The local and systemic T-cell response to Helicobacter pylori in gastric cancer patients is characterised by production of interleukin-10. *Clin Immunol* 125:205-213.

62. Vogl, F. D., M. Frey, R. Kreienberg, and I. B. Runnebaum. 2000. Autoimmunity against p53 predicts invasive cancer with poor survival in patients with an ovarian mass. *Br J Cancer* 83:1338-1343.

63. Abendstein, B., C. Marth, E. Muller-Holzner, M. Widschwendter, G. Daxenbichler, and A. G. Zeimet. 2000. Clinical significance of serum and ascitic p53 autoantibodies in epithelial ovarian carcinoma. *Cancer* 88:1432-1437.

64. Bergqvist, A. S., M. Bergqvist, D. Brattstrom, P. Hesselius, A. Larsson, O. Brodin, and G. Wagenius. 2001. Serum p53 autoantibodies as prognostic marker in patients with oesophageal carcinoma. *Anticancer Res* 21:4141-4145.

65. Gumus, E., S. Erdamar, G. Demirel, K. Horasanli, M. Kendirci, and C. Miroglu. 2004. Association of positive serum anti-p53 antibodies with poor prognosis in bladder cancer patients. *Int J Urol* 11:1070-1077.

66. Mack, U., D. Ukena, M. Montenarh, and G. W. Sybrecht. 2000. Serum anti-p53 antibodies in patients with lung cancer. *Oncol Rep* 7:669-674.

67. Pallasch, C. P., A. K. Struss, A. Munnia, J. Konig, W. I. Steudel, U. Fischer, and E. Meese. 2005. Autoantibodies against GLEA2 and PHF3 in glioblastoma: tumor-associated autoantibodies correlated with prolonged survival. *Int J Cancer* 117:456-459.

68. Bachelot, T., D. Ratel, C. Menetrier-Caux, D. Wion, J. Y. Blay, and F. Berger. 2006. Autoantibodies to endostatin in patients with breast cancer: correlation to endostatin levels and clinical outcome. *Br J Cancer* 94:1066-1070.

69. Gogas, H., J. Ioannovich, U. Dafni, C. Stavropoulou-Giokas, K. Frangia, D. Tsoutsos, P. Panagiotou, A. Polyzos, O. Papadopoulos, A. Stratigos, C. Markopoulos, D. Bafaloukos, D. Pectasides, G. Fountzilas, and J. M. Kirkwood. 2006. Prognostic significance of autoimmunity during treatment of melanoma with interferon. *N Engl J Med* 354:709-718.

70. Satzger, I., A. Meier, F. Schenck, A. Kapp, A. Hauschild, and R. Gutzmer. 2007. Autoimmunity as a prognostic factor in melanoma patients treated with adjuvant low-dose interferon alpha. *Int J Cancer* 121:2562-2566.

71. Xue, L. J., Q. S. Su, J. H. Yang, and Y. Lin. 2008. Autoimmune responses induced by Helicobacter pylori improve the prognosis of gastric carcinoma. *Med Hypotheses* 70:273-276.